Bahnen und Schwere

Adrian Jäggi

AIUB

Astronomical Institute
University of Bern

GOCE Orbit Characteristics (1)

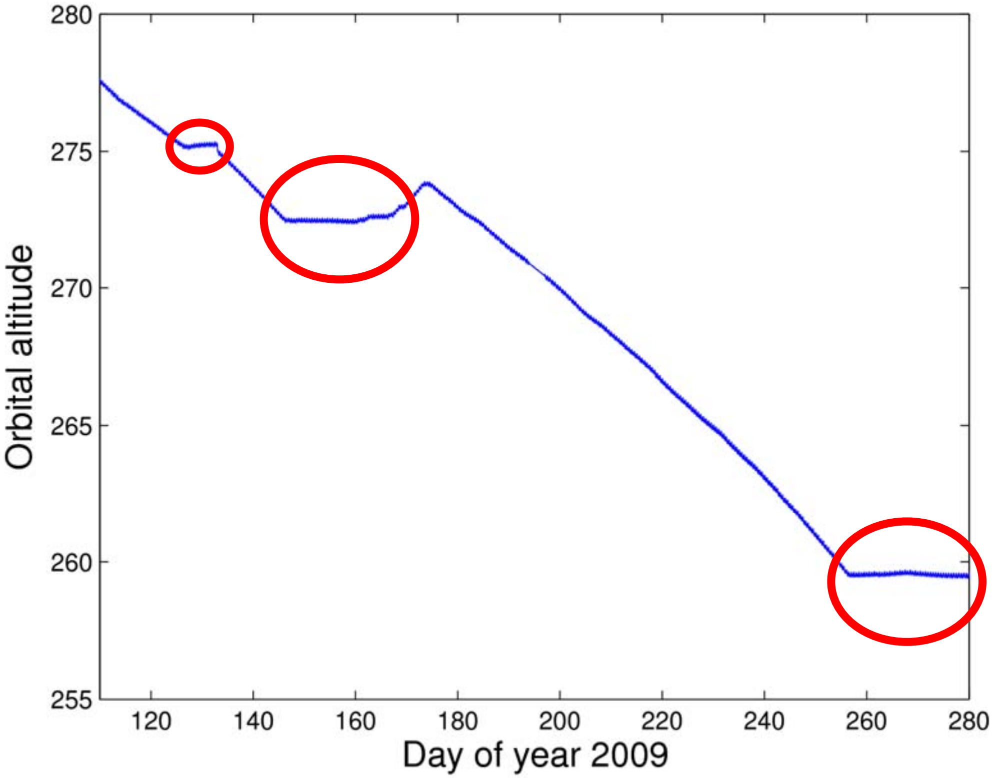

GOCE „History“:

17 March:
Launch into a sun-synchronous (i ~ 97°), dusk-dawn orbit at an altitude of 287.9 km

7 May:
First drag-free flight

26 May:
Second drag-free flight with various activities on gradiometer calibration

13/14 September:
Arrival at final orbital altitude of 259.6 km (254.9 km), start of drag-free flight for first Measurement and Operational Phase (MOP-1)

GOCE Orbit Characteristics (2)

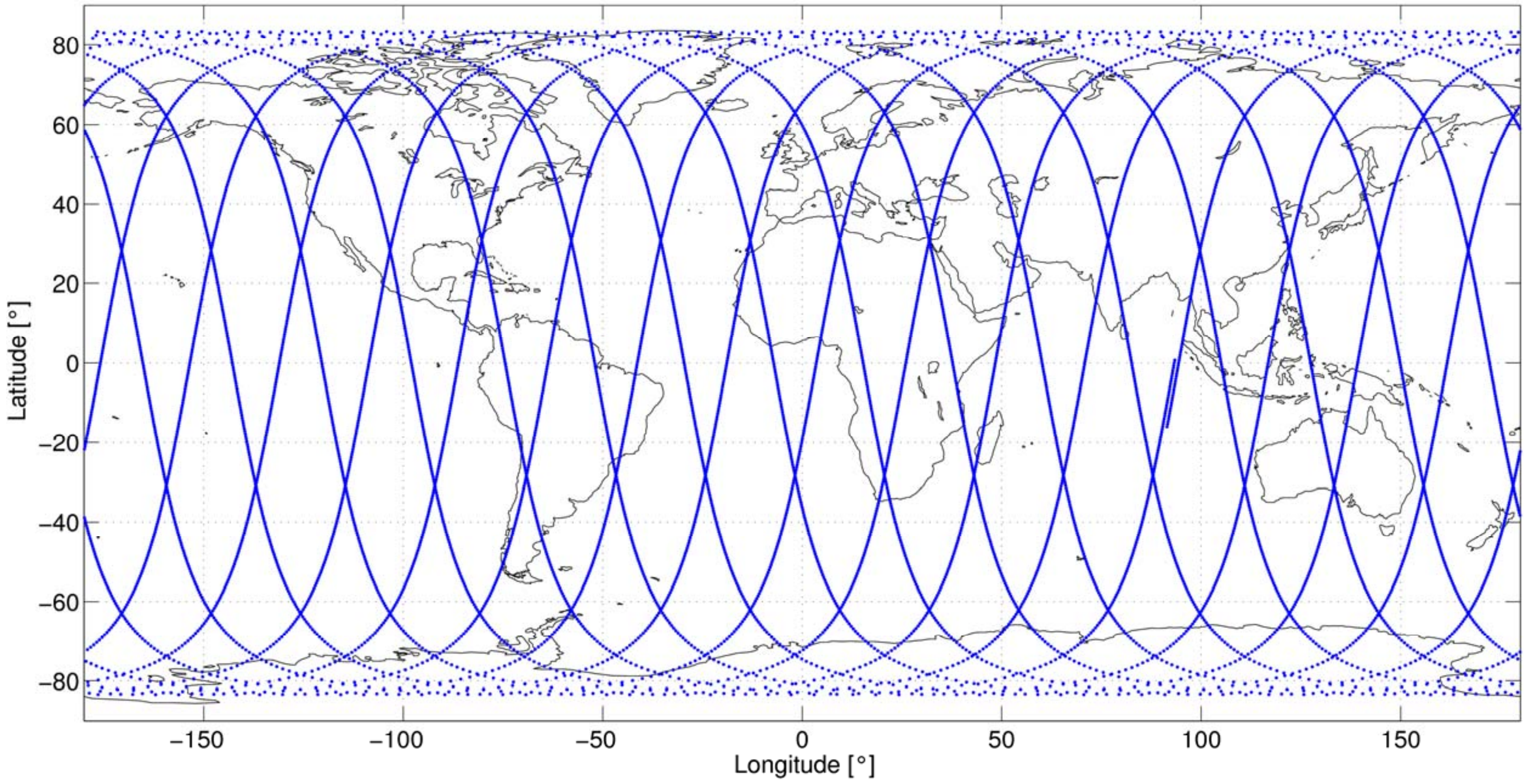

Ground-track coverage on 2 Nov, 2009

Complete geographical coverage after 979 revolutions (repeat-cycle of 61 days)

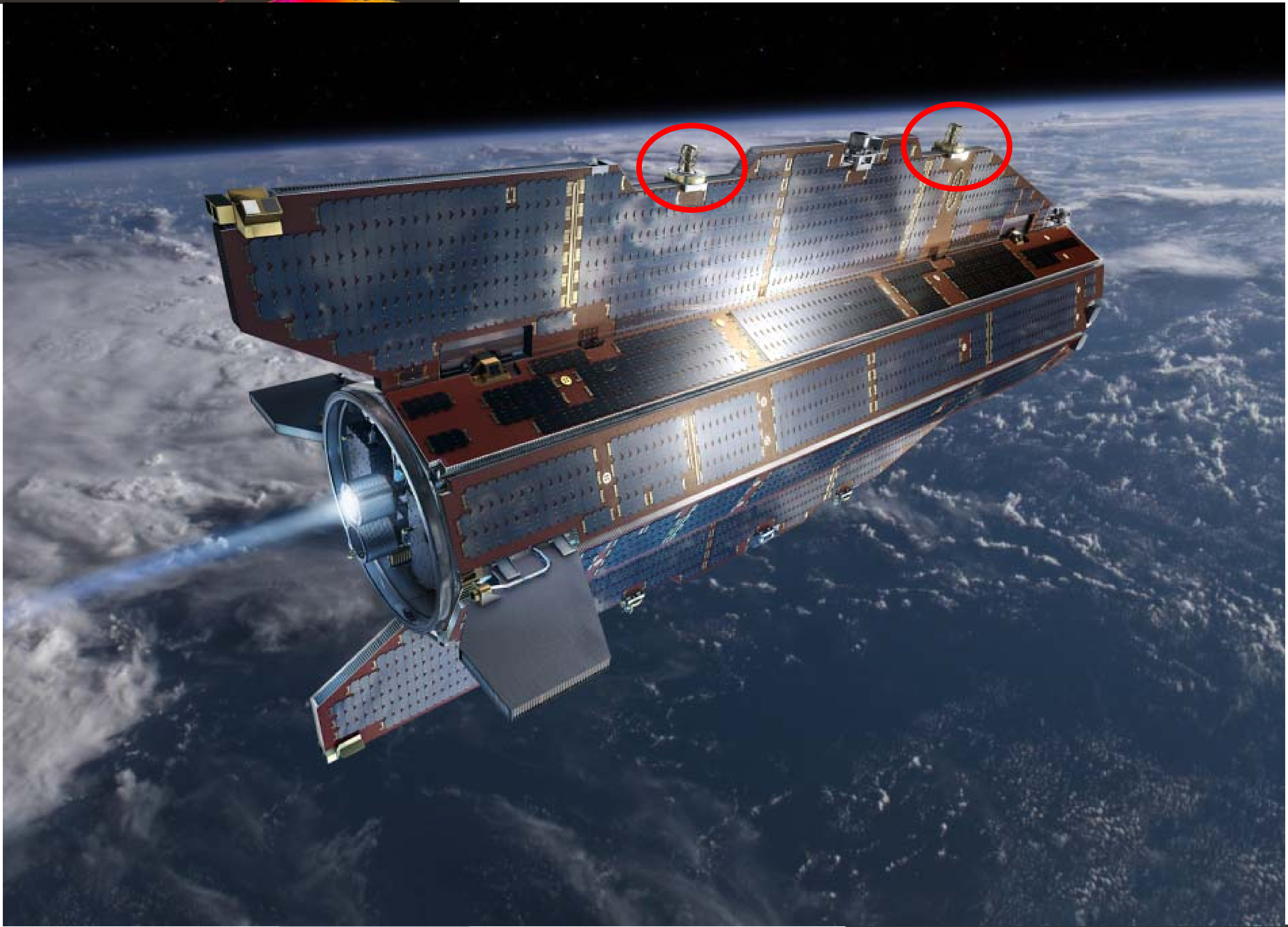

Introduction to GPS

GPS: **G**lobal **P**ositioning **S**ystem

Characteristics:

- Satellite system for (real-time) **Positioning** and **Navigation**
- **Global** (everywhere on Earth, up to altitudes of 5000km) and **at any time**
- **Unlimited** number of users
- **Weather-independent** (radio signals are passing through the atmosphere)
- **3-dimensional position**, **velocity** and **time** information

GPS Segments

The GPS consists of **3 main segments**:

- **Space Segment**: the satellites and the constellation of satellites

- **Control Segment**: the ground stations, infrastructure and software for operation and monitoring of the GPS

- **User Segment**: all GPS receivers worldwide and the corresponding processing software

We should add an important **4th segment**:

- **Ground Segment**: all civilian permanent networks of reference sites and the international/regional/local services delivering products for the users

Space Segment

- The space segment nominally consists of **24 satellites**, presently: **30** active GPS satellites

- Constellation design: at least **4 satellites** in view from **any location** on the Earth at **any time**

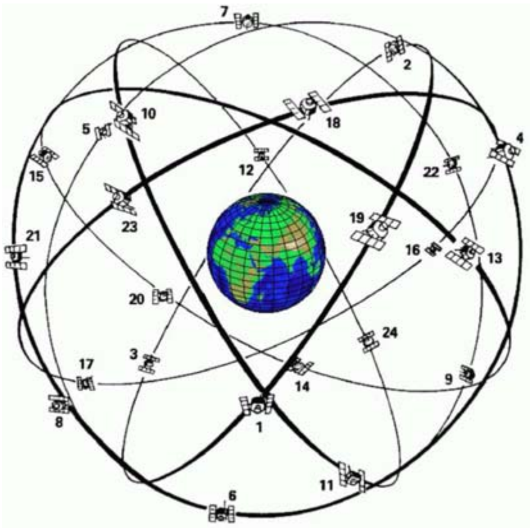

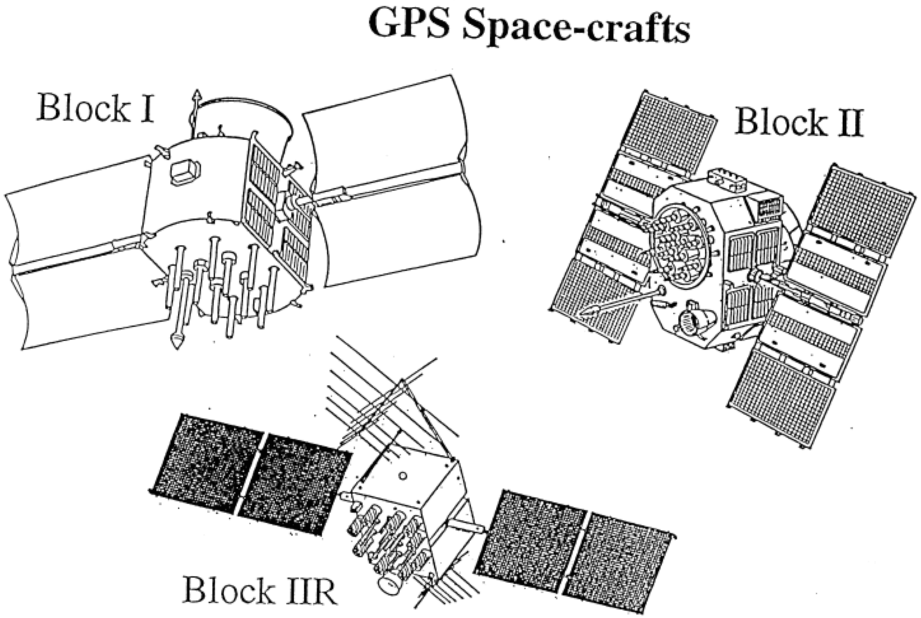

Control Segment

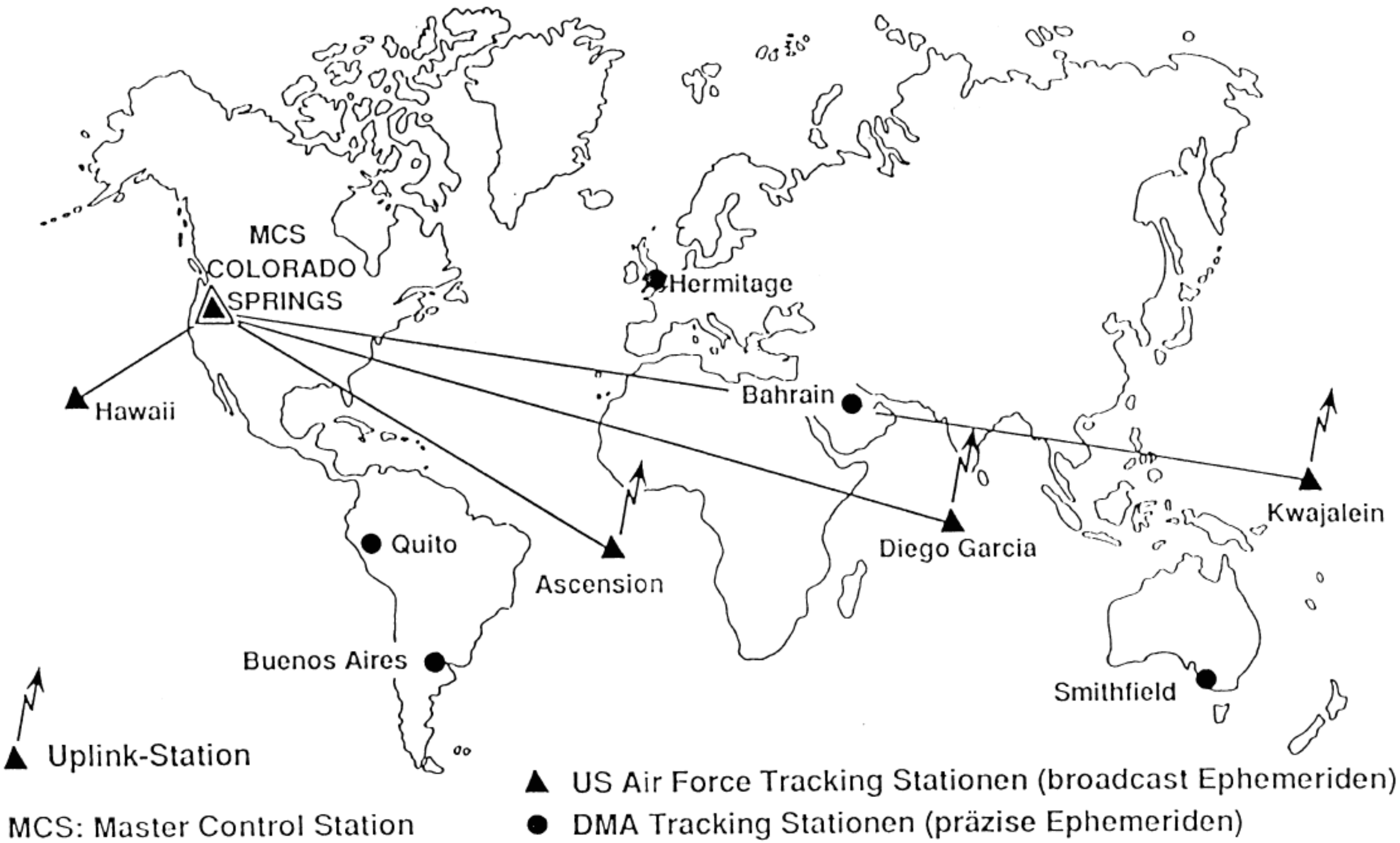

User Segment and Ground Segment

User Segment:

- All **GPS receivers** on land, on sea, in the air and in space
- Broad user community with applications of the GPS for positioning and navigation, surveying, geodynamics and geophysics, atmosphere, …

Ground Segment:

- Global network of the International GNSS Service (IGS: ~ 400 stations)
- Regional and local permanent networks (Europe, Japan, US): densification of the reference frame, positioning services

Global Network of the IGS

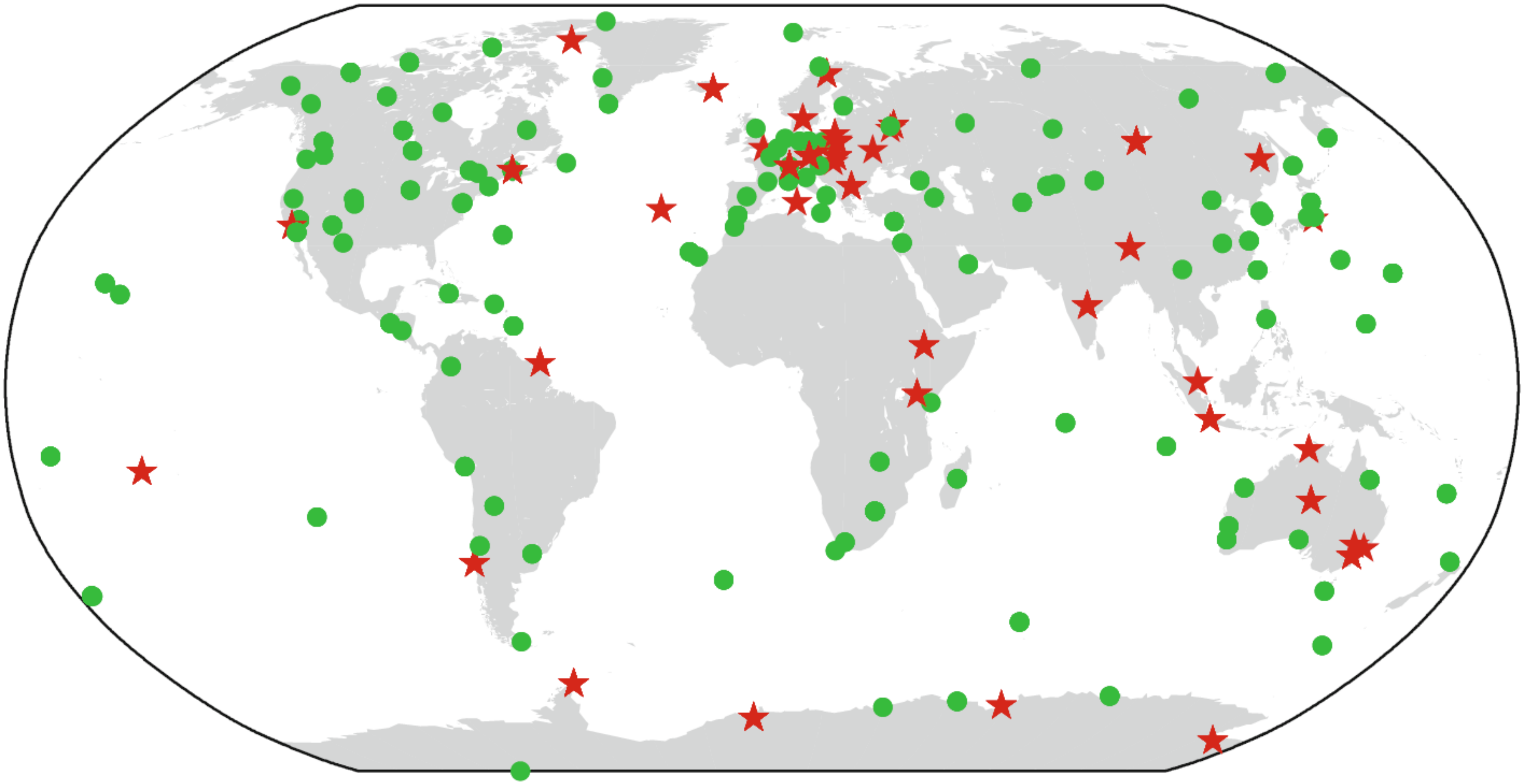

● GPS-only receivers
★ Combined GPS-GLONASS receivers

IGS stations used for computation of final orbits at CODE (Dach et al., 2009)

Analysis Centers (ACs) of the IGS

CODE (Center for Orbit Determination in Europe):

CODE is a joint-venture between:

- Astronomical Institute of the University of Bern (AIUB), Bern, Switzerland
- Swiss Federal Office of Topography (swisstopo), Wabern, Switzerland
- German Federal Office for Cartography and Geodesy (BKG), Frankfurt, Germany
- Institute of Astronomical and Physical Geodesy (IAPG) of the Technische Universität München (TUM), Munich, Germany

AIUB

Schweizerische Eidgenossenschaft
Confédération suisse
Confederazione Svizzera
Confederaziun svizra

Bundesamt für Kartographie und Geodäsie

Technische Universität München

Computation of Final Orbits at CODE

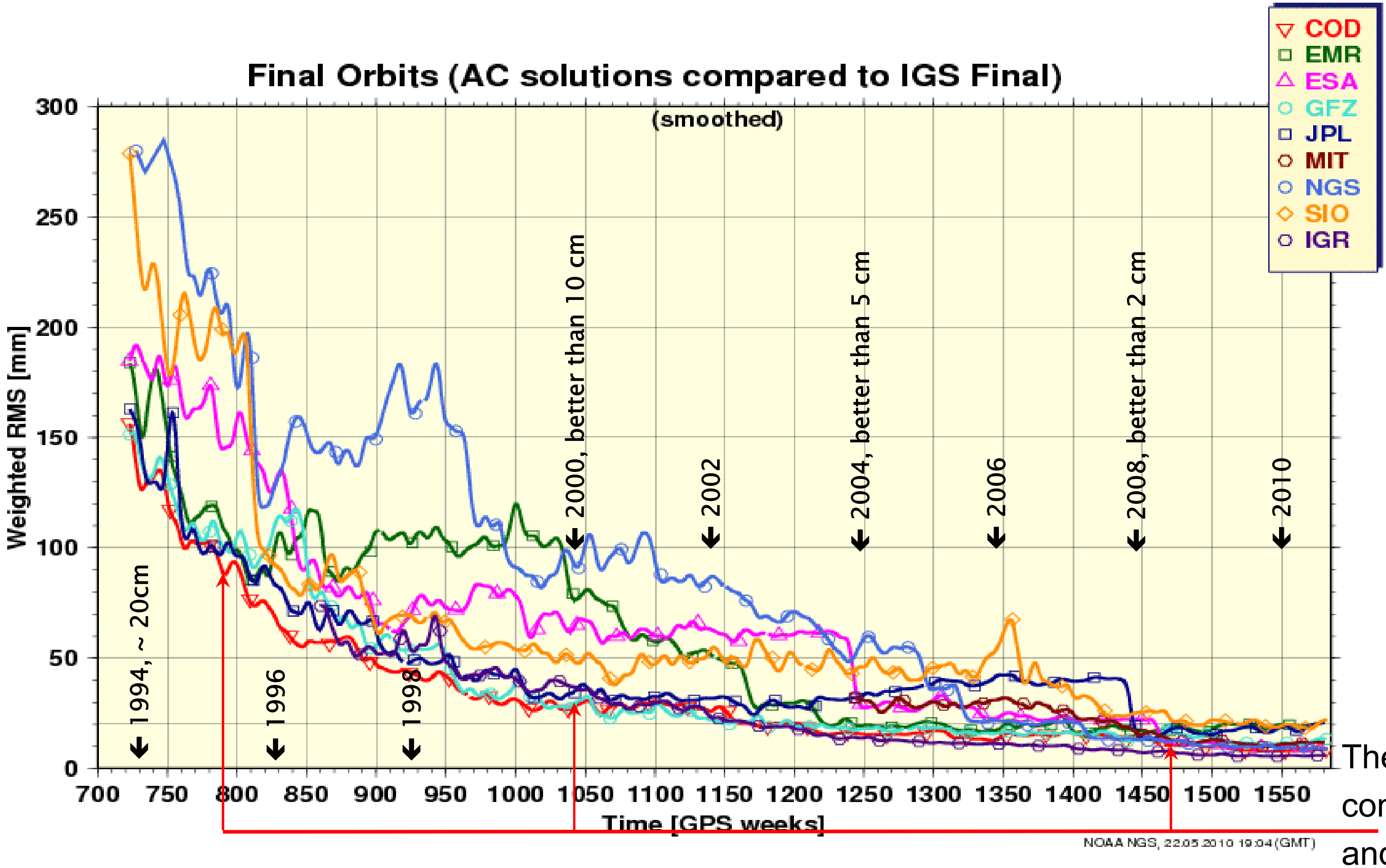

The COD solution is computed at AIUB and used for GOCE orbit determination

Computation of Final Clocks at CODE

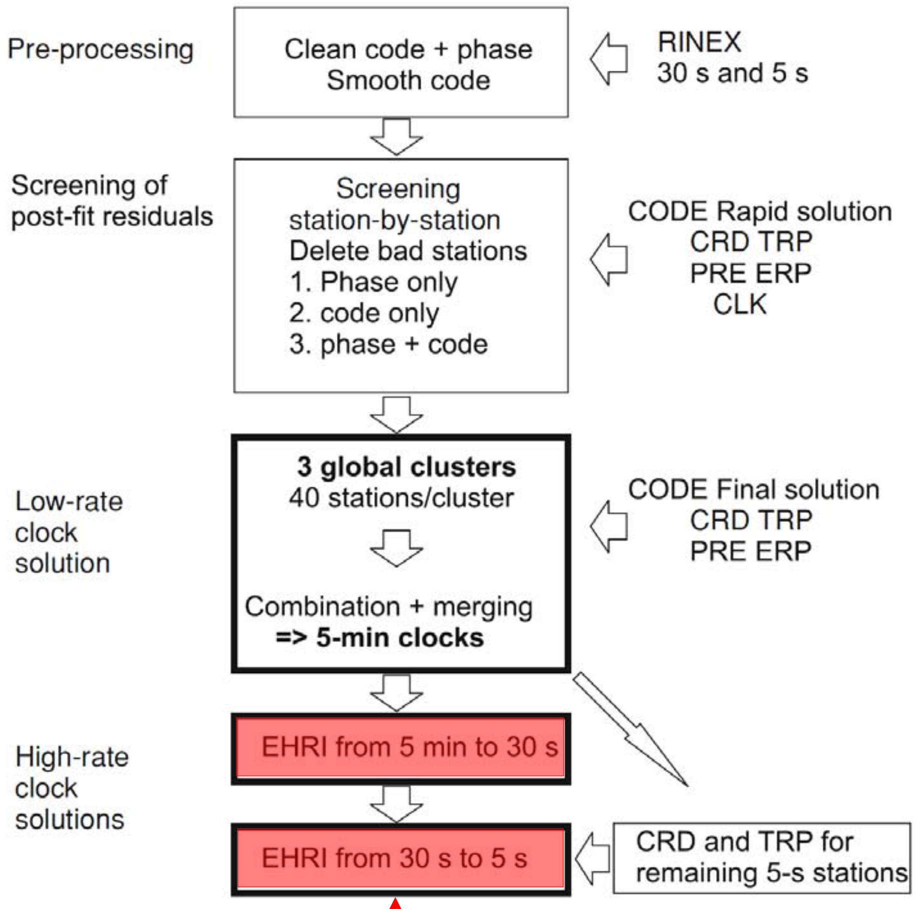

(Bock et al., 2009)

The final clock product with 5 min sampling is based on undifferenced GPS data of at maximum 120 stations of the IGS network

The IGS 1 Hz network is finally used for clock densification to 5 sec

The 5 sec clocks are interpolated to 1 sec as needed for GOCE orbit determination

GPS Signals

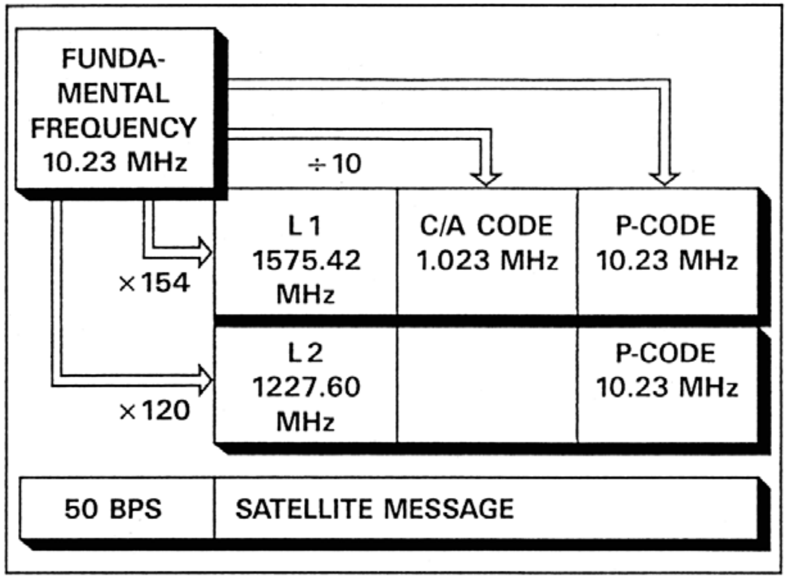

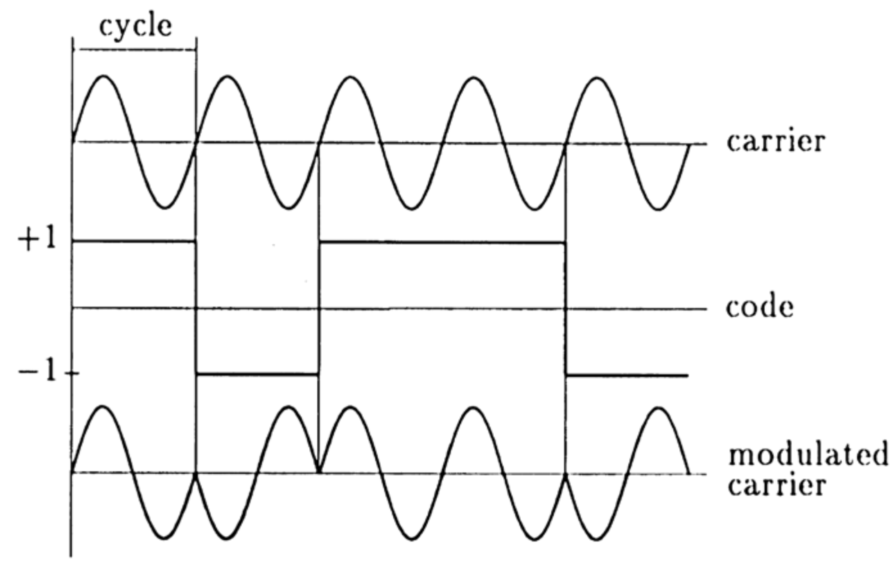

Signals driven by an **atomic clock**

Two **carrier signals** (sine waves):

- **L1**: f = 1575.43 MHz, λ = 19 cm
- **L2**: f = 1227.60 MHz, λ = 24 cm

Bits encoded on carrier by phase modulation:

- **C/A-code** (Clear Access / Coarse Acquisition)
- **P-code** (Protected / Precise)
- **Broadcast/Navigation Message**

Pseudorange / Code Measurements

Code Observations P_i^k are defined as:

$$P_i^k \doteq c\,(T_i - T^k)$$

c	Speed of light (in vacuum)
T_i	Receiver clock reading at signal reception (in receiver clock time)
T^k	GPS satellite clock reading at signal emission (in satellite clock time)

- No actual „**range**“ (distance) because of clock offsets
- **Measurement noise**: ~ 0.5 m for GOCE P-code

Code Observation Equation

$$P_i^k = \rho_i^k - c \cdot \Delta t^k + c \cdot \Delta t_i$$

t_i, t^k	GPS time of reception and emission
Δt^k	Satellite clock offset $T^k - t^k$
Δt_i	Receiver clock offset $T_i - t_i$
ρ_i^k	Distance between receiver and satellite $c\,(t_i - t^k)$

Known from ACs or IGS:

- satellite positions $(x^{k_j}, y^{k_j}, z^{k_j})$
- satellite clock offsets Δt^{k_j}

4 unknown parameters:

- receiver position (x_i, y_i, z_i)
- receiver clock offset Δt_i

Basic Positioning and Navigation Concept (1)

Simplified model for ρ_i^k: atmospheric delay missing, exactly 4 satellites, …

$$P_i^{k_1} = \sqrt{(x^{k_1} - x_i)^2 + (y^{k_1} - y_i)^2 + (z^{k_1} - z_i)^2} - c \cdot \Delta t^{k_1} + c \cdot \Delta t_i$$

$$P_i^{k_2} = \sqrt{(x^{k_2} - x_i)^2 + (y^{k_2} - y_i)^2 + (z^{k_2} - z_i)^2} - c \cdot \Delta t^{k_2} + c \cdot \Delta t_i$$

$$P_i^{k_3} = \sqrt{(x^{k_3} - x_i)^2 + (y^{k_3} - y_i)^2 + (z^{k_3} - z_i)^2} - c \cdot \Delta t^{k_3} + c \cdot \Delta t_i$$

$$P_i^{k_4} = \sqrt{(x^{k_4} - x_i)^2 + (y^{k_4} - y_i)^2 + (z^{k_4} - z_i)^2} - c \cdot \Delta t^{k_4} + c \cdot \Delta t_i$$

More than 4 satellites: best receiver position and clock offset with **least-squares** or **filter** algorithms

Basic Positioning and Navigation Concept (2)

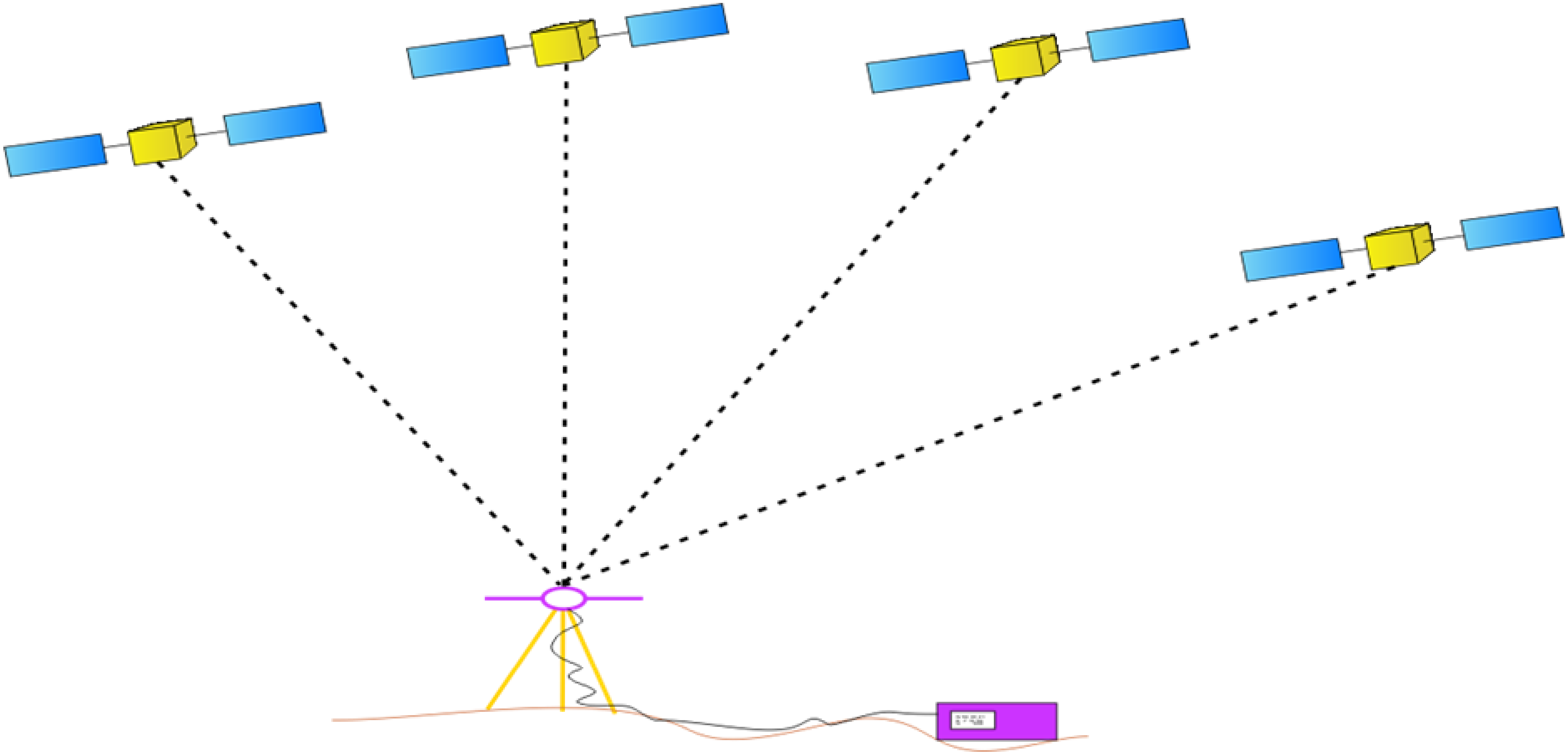

Carrier Phase Measurements (1)

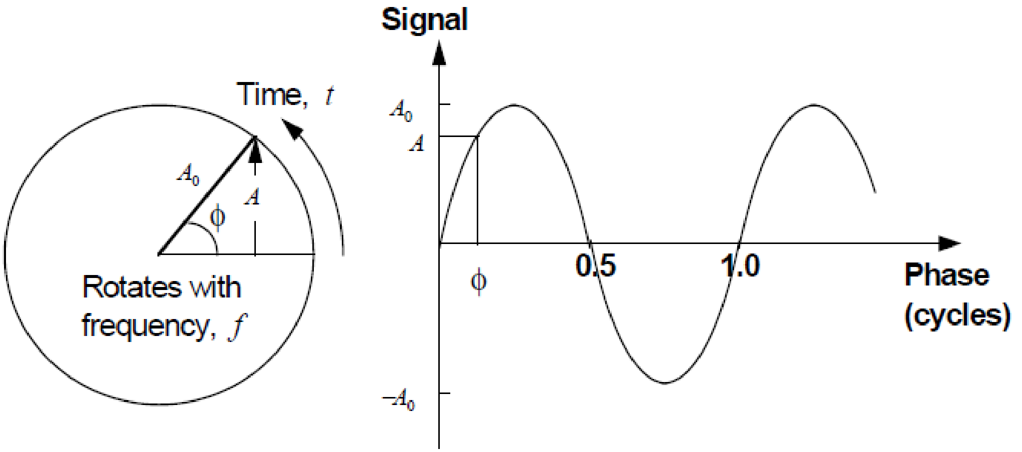

Phase ϕ (in cycles) increases linearly with time t:

$$\phi = f \cdot t$$

where f is the frequency

The **satellite** generates with its clock the phase signal ϕ^k. At emmision time T^k (in satellite clock time) we have

$$\phi^k = f \cdot T^k$$

The same phase signal, e.g., a wave crest, propagates from the satellite to the receiver, but the receiver measures only the fractional part of the phase and does not know the **integer number of cycles** N_i^k (phase ambiguity):

$$\phi_i^k = \phi^k - N_i^k = f \cdot T^k - N_i^k$$

Carrier Phase Measurements (2)

The **receiver** generates with its clock a **reference phase**. At time of reception T_i of the satellite phase ϕ_i^k (in receiver clock time) we have:

$$\phi_i = f \cdot T_i$$

The actual **phase measurement** is the difference between receiver reference phase ϕ_i and satellite phase ϕ_i^k:

$$\psi_i^k = \phi_i - \phi_i^k = f \cdot T_i - (f \cdot T^k - N_i^k) = f \cdot (T_i - T^k) + N_i^k$$

Multiplication with the wavelength $\lambda = c/f$ leads to the **phase observation equation** in meters:

$$\begin{aligned} L_i^k &= \lambda \cdot \psi_i^k = c \cdot (T_i - T^k) + \lambda \cdot N_i^k \\ &= \rho_i^k - c \cdot \Delta t^k + c \cdot \Delta t_i + \lambda \cdot N_i^k \end{aligned}$$

Difference to the pseudorange observation: **integer ambiguity term** N_i^k

Improved Observation Equation

$$L_i^k = \rho_i^k - c \cdot \Delta t^k + c \cdot \Delta t_i + \cancel{T_i^k} + \cancel{I_i^k} + \lambda \cdot N_i^k$$
$$+ \Delta_{rel} - c \cdot b^k + c \cdot b_i + m_i^k + \epsilon_i^k$$

ρ_i^k	Distance between satellite and receiver	Satellite positions and clocks
Δt^k	Satellite clock offset wrt GPS time	are known from ACs or IGS
Δt_i	Receiver clock offset wrt GPS time	
~~T_i^k~~	~~Tropospheric delay~~	Not existent for LEOs
~~I_i^k~~	~~Ionospheric delay~~	Cancels out (first order only) when forming the ionosphere-free linear combination:
N_i^k	Phase ambiguity	
Δ_{rel}	Relativistic corrections	
b^k	Delays in satellite (cables, electronics)	
b_i	Delays in receiver and antenna	
m_i^k	Multipath, scattering, bending effects	
ϵ_i^k	Measurement error	

$$L_c = \frac{f_1^2}{f_1^2 - f_2^2} L_1 - \frac{f_2^2}{f_1^2 - f_2^2} L_2$$

Time Systems and Reference Systems

Time Systems:

- **TAI** (Temps Atomic International): ensemble of atomic clocks
- **UT1** (Universal Time 1): time defined by the Earth‘s rotation
- **UTC** (Universal Time Coordinated): differs from TAI only by leap seconds (adjusted to UT1: $|UT1 – UTC| < 0.9$ sec)
- **GPS time**: constant difference **TAI - GPS = 19 sec**
- **GPS-UTC = 15 sec** at present

Reference Systems:

- ITRF (International Terrestrial Reference Frame): combination of global VLBI, SLR, GPS and DORIS solutions. Best Earth-fixed reference frame, at present still ITRF2005
- ICRF (International Celestial Reference Frame): inertial frame, realized by coordinates of extragalactic radio sources

(GOCE Standards, 2009)

Geometric Distance

Geometric distance ρ_{leo}^k is given by:

$$\rho_{leo}^k = \left|\boldsymbol{r}_{leo}(t_{leo}) - \boldsymbol{r}^k(t_{leo} - \tau_{leo}^k)\right|$$

$\boldsymbol{r}_{leo}$	Inertial position of LEO antenna phase center at reception time
$\boldsymbol{r}^k$	Inertial position of GPS antenna phase center of satellite k at emission time
τ_{leo}^k	Signal traveling time between the two phase center positions

Different ways to represent $\boldsymbol{r}_{leo}$:

- **Kinematic** orbit representation
- **Dynamic** or **reduced-dynamic** orbit representation

Kinematic Orbit Representation (1)

Satellite position $\boldsymbol{r}_{leo}(t_{leo})$ (in inertial frame) is given by:

$$\boldsymbol{r}_{leo}(t_{leo}) = \boldsymbol{R}(t_{leo}) \cdot (\boldsymbol{r}_{leo,e,0}(t_{leo}) + \delta\boldsymbol{r}_{leo,e,ant}(t_{leo}))$$

$\boldsymbol{R}$	Transformation matrix from Earth-fixed to inertial frame
$\boldsymbol{r}_{leo,e,0}$	LEO center of mass position in Earth-fixed frame
$\delta\boldsymbol{r}_{leo,e,ant}$	LEO antenna phase center offset in Earth-fixed frame

Kinematic positions $\boldsymbol{r}_{leo,e,0}$ are estimated for each **measurement epoch**:

- Measurement epochs **need not** to be identical with nominal epochs
- Positions are **independent** of models describing the LEO dynamics
  Velocities cannot be provided

Kinematic Orbit Representation (2)

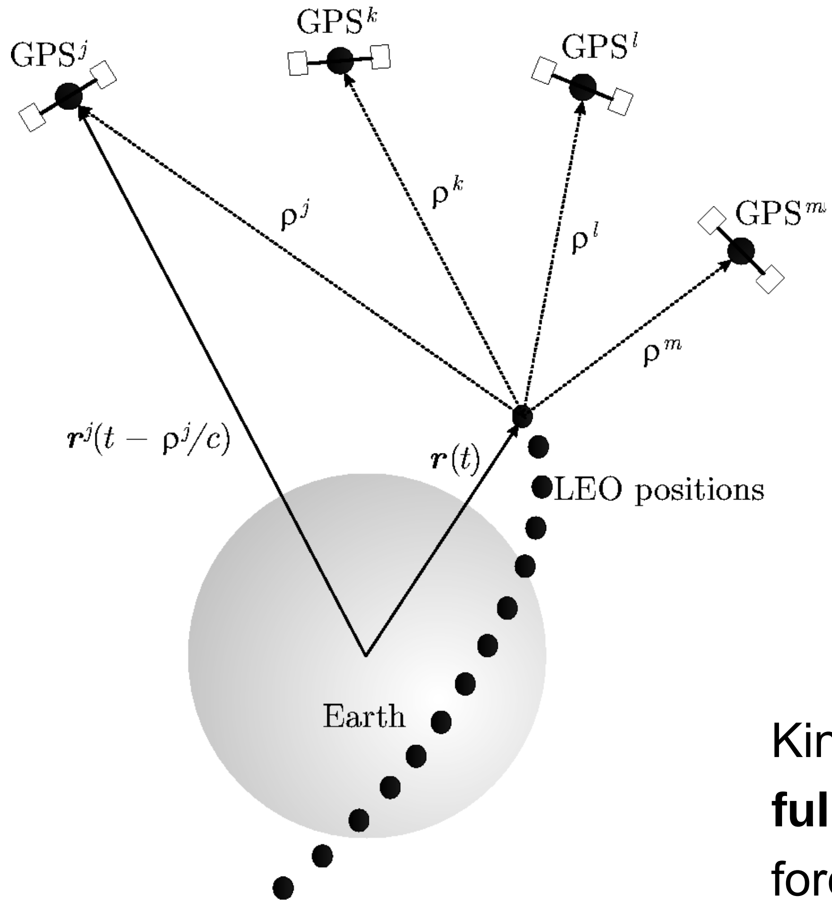

A kinematic orbit is an ephemeris at **discrete** measurement epochs

Kinematic positions are **fully independent** on the force models used for LEO orbit determination

(Svehla and Rothacher, 2004)

Kinematic Orbit Representation (3)

Measurement epochs
(in GPS time)

Positions (km)
(Earth-fixed)

Clock correction to nominal epoch (μs), e.g., to epoch 00:00:03

```
*  2009 11  2  0  0  0.80678020
PL15  -390.612059  6623.987679    73.104149 193219.797196
*  2009 11  2  0  0  1.80678020
PL15  -389.240315  6624.166512    65.402457 193219.799413
*  2009 11  2  0  0  2.80678020
PL15  -387.868014  6624.336133    57.700679 193219.801634
*  2009 11  2  0  0  3.80678020
PL15  -386.495163  6624.496541    49.998817 193219.803855
*  2009 11  2  0  0  4.80678019
PL15  -385.121760  6624.647724    42.296889 193219.806059
*  2009 11  2  0  0  5.80678019
PL15  -383.747819  6624.789703    34.594896 193219.808280
*  2009 11  2  0  0  6.80678019
PL15  -382.373332  6624.922464    26.892861 193219.810495
*  2009 11  2  0  0  7.80678019
PL15  -380.998306  6625.046003    19.190792 193219.812692
*  2009 11  2  0  0  8.80678019
PL15  -379.622745  6625.160329    11.488692 193219.814899
*  2009 11  2  0  0  9.80678018
PL15  -378.246651  6625.265448     3.786580 193219.817123
```

Excerpt of kinematic GOCE positions at begin of 2 Nov, 2009

GO_CONS_SST_PKI_2__20091101T235945_20091102T235944_0001 Times in UTC

Measurement Epochs

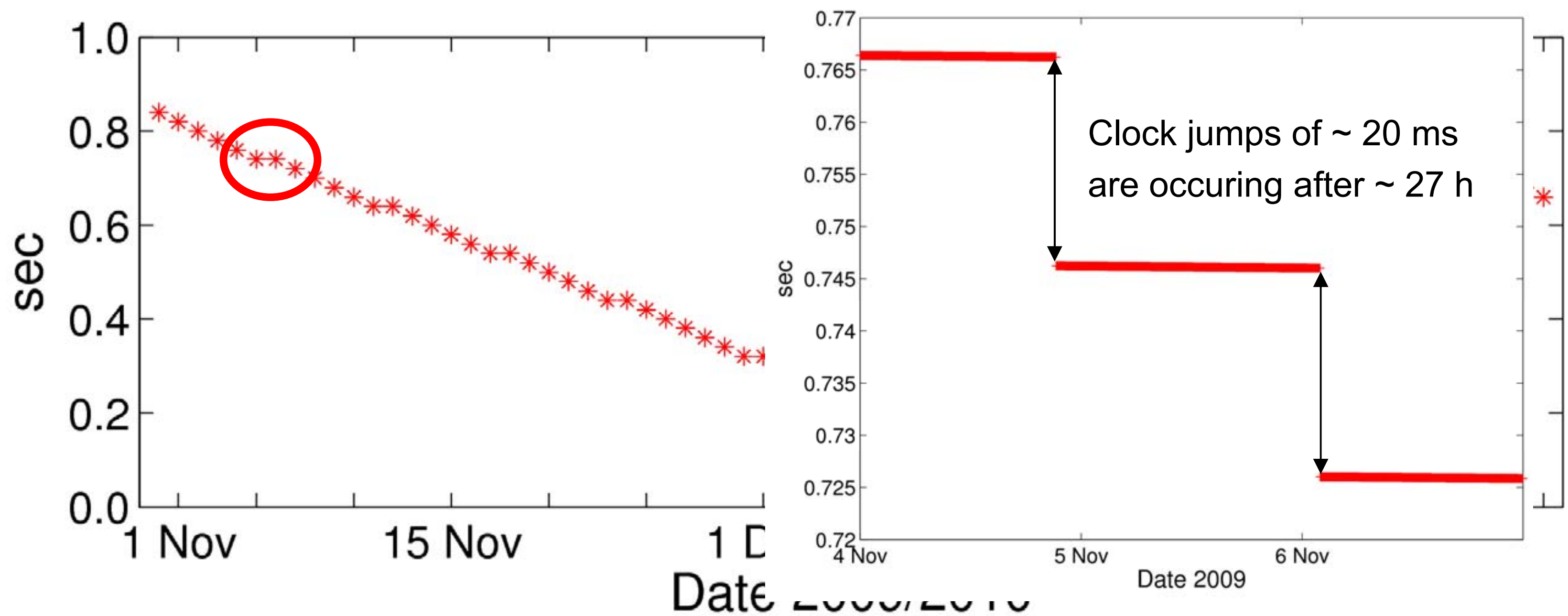

Fractional parts of measurement epochs:

The measurement sampling is 1 Hz, but the internal clock is not steered to integer seconds (fractional parts are shown in the figure for the midnight epochs).

Dynamic Orbit Representation (1)

Satellite position $\boldsymbol{r}_{leo}(t_{leo})$ (in inertial frame) is given by:

$$\boldsymbol{r}_{leo}(t_{leo}) = \boldsymbol{r}_{leo,0}(t_{leo}; a, e, i, \Omega, \omega, u_0; Q_1, ..., Q_d) + \delta\boldsymbol{r}_{leo,ant}(t_{leo})$$

$\boldsymbol{r}_{leo,0}$	LEO center of mass position
$\delta\boldsymbol{r}_{leo,ant}$	LEO antenna phase center offset
$a, e, i, \Omega, \omega, u_0$	LEO initial osculating orbital elements
$Q_1, ..., Q_d$	LEO dynamical parameters

Satellite trajectory $\boldsymbol{r}_{leo,0}$ is a particular solution of an **equation of motion**

- One set of **initial conditions** (orbital elements) is estimated per arc
  Dynamical parameters of the force model on request

Dynamic Orbit Representation (2)

Equation of motion (in inertial frame) is given by:

$$\ddot{\boldsymbol{r}} = -GM\frac{\boldsymbol{r}}{r^3} + \boldsymbol{f}_1(t, \boldsymbol{r}, \dot{\boldsymbol{r}}, Q_1, ..., Q_d)$$

with initial conditions

$$\boldsymbol{r}(t_0) = \boldsymbol{r}(a, e, i, \Omega, \omega, u_0; t_0)$$
$$\dot{\boldsymbol{r}}(t_0) = \dot{\boldsymbol{r}}(a, e, i, \Omega, \omega, u_0; t_0)$$

The **acceleration** $\boldsymbol{f}_1$ consists of **gravitational** and **non-gravitational** perturbations taken into account to model the satellite trajectory. Unknown parameters $Q_1, ..., Q_d$ of force models may appear in the equation of motion together with deterministic (known) accelerations given by analytical models.

Osculating Orbital Elements (1)

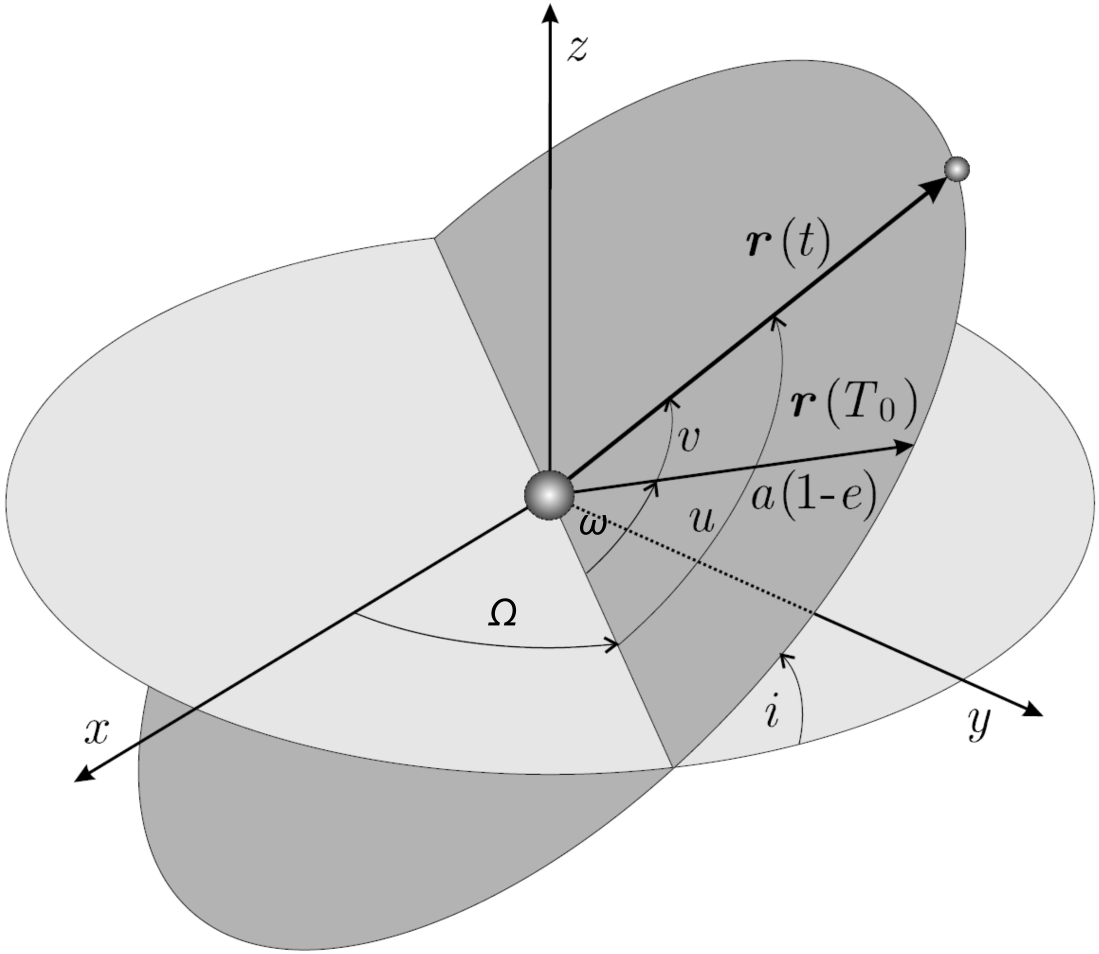

Osculating Orbital Elements of GOCE (2)

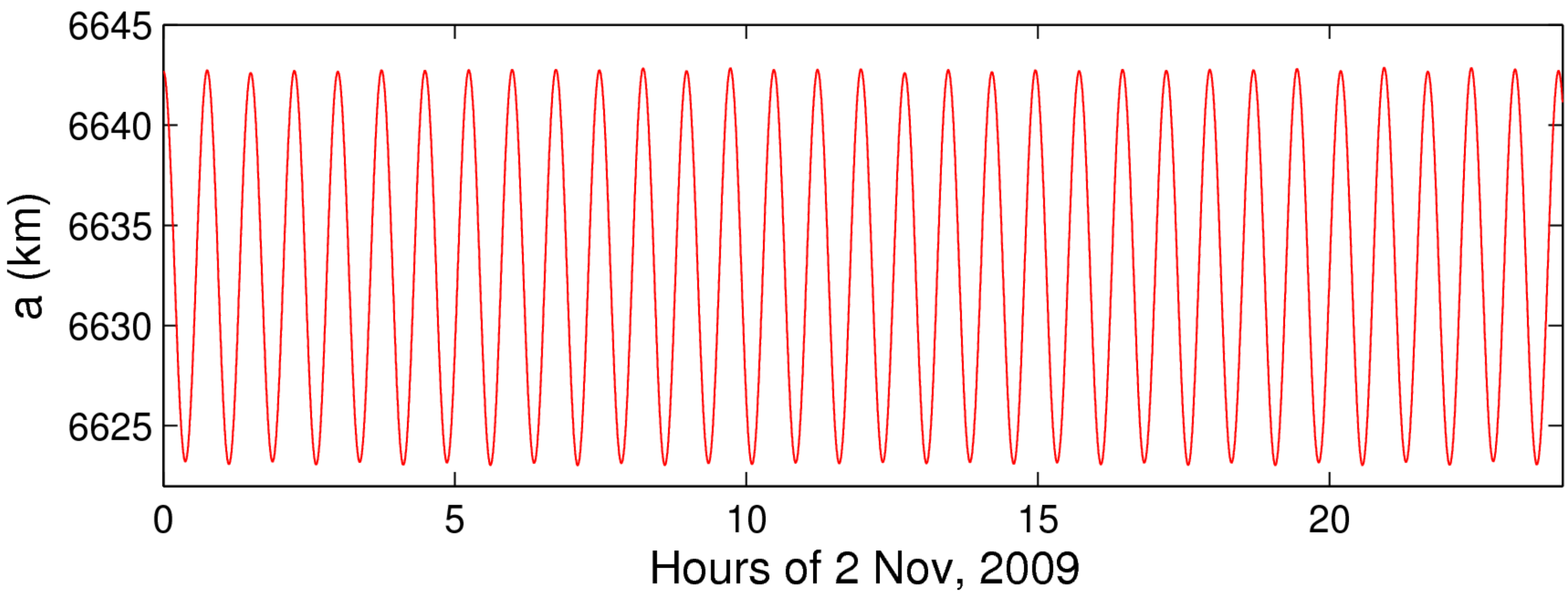

Semi-major axis:
Twice-per-revolution variations of about ±10 km around the mean semi-major axis of 6632.9km, which corresponds to the 254.9 km mean altitude used by ESA

Osculating Orbital Elements of GOCE (3)

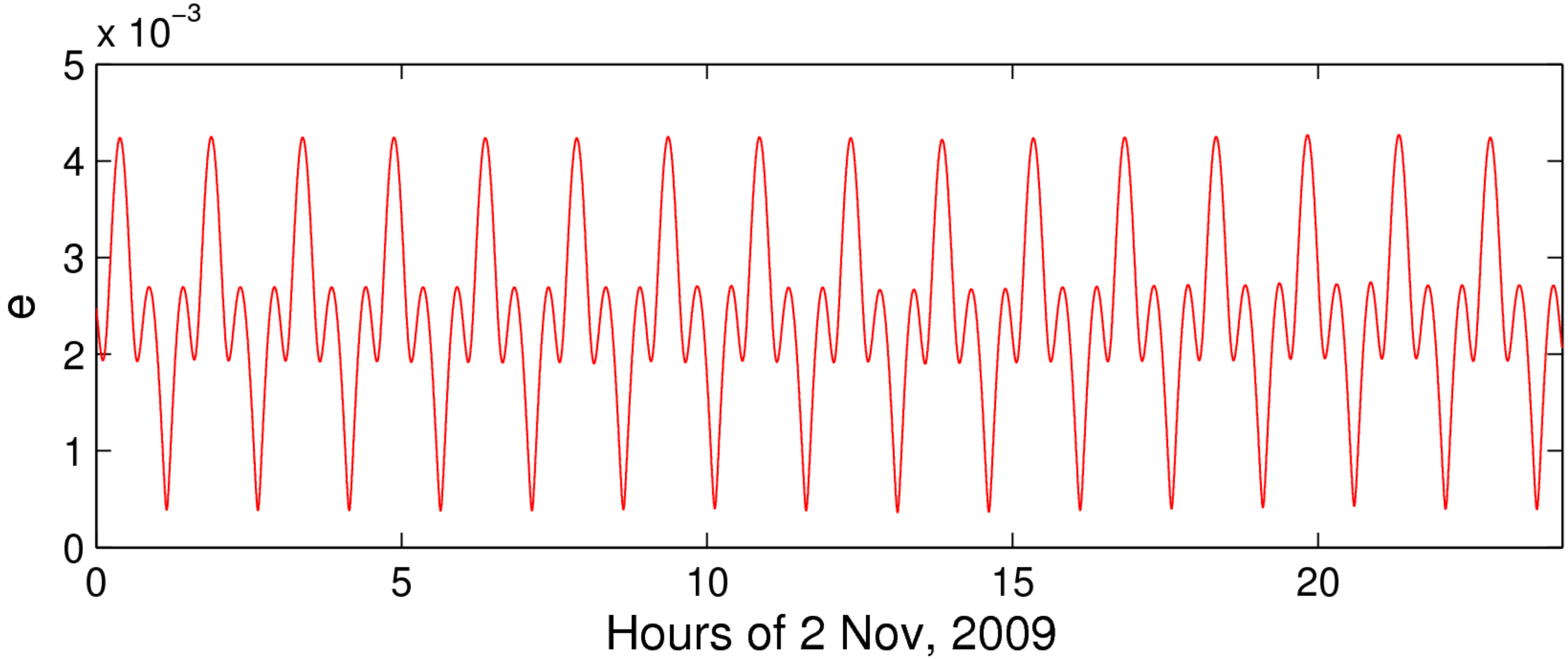

Numerical eccentricity:

Small, short-periodic variations around the mean value of about 0.0025, i.e., the orbit is close to circular

Osculating Orbital Elements of GOCE (4)

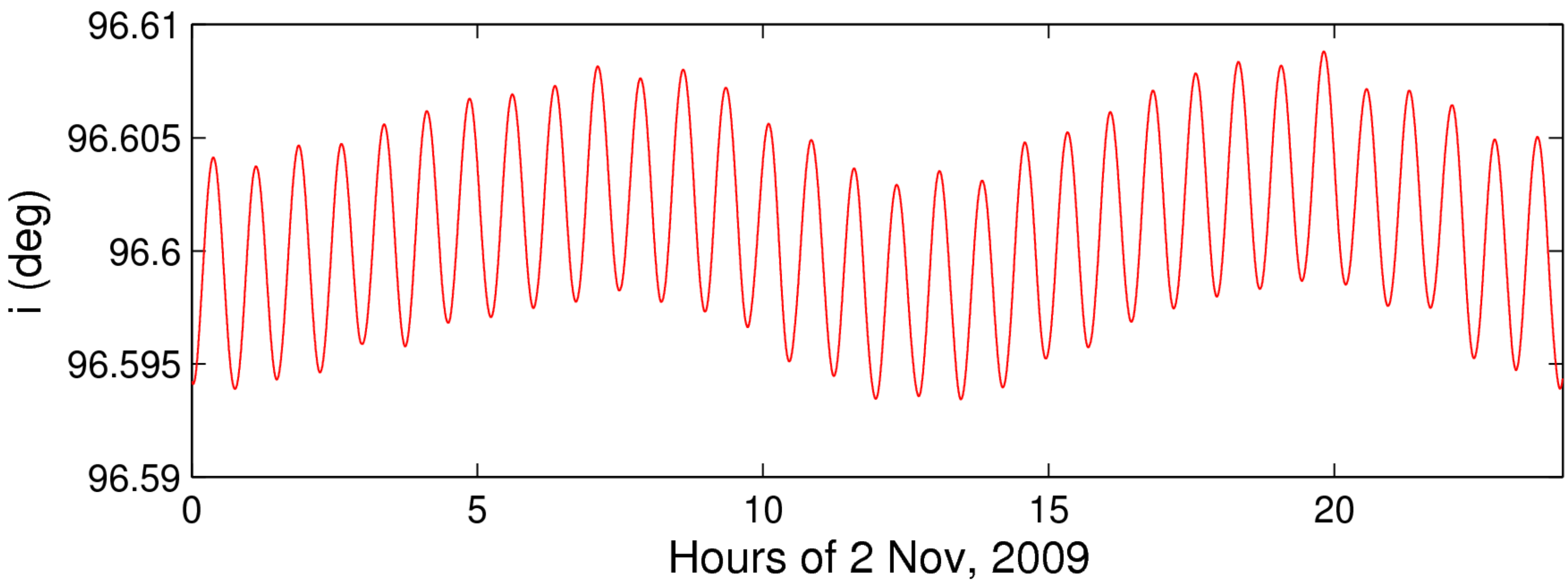

Inclination:

Twice-per-revolution and longer variations around the mean inclination of about 96.6° (sun-synchronous orbit)

Osculating Orbital Elements of GOCE (5)

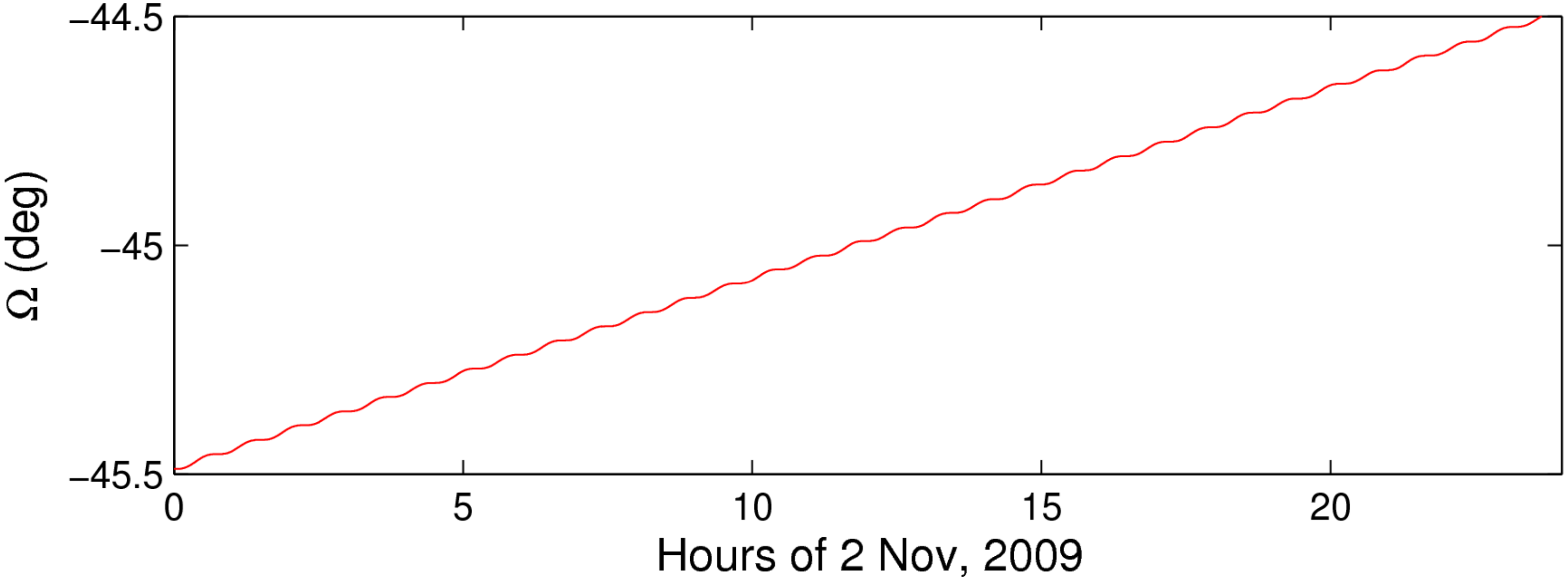

Right ascension of ascending node:

Twice-per-revolution variations and linear drift of about +1°/day (360°/365days) due to the sun-synchronous orbit

Dynamic Orbit Representation (3)

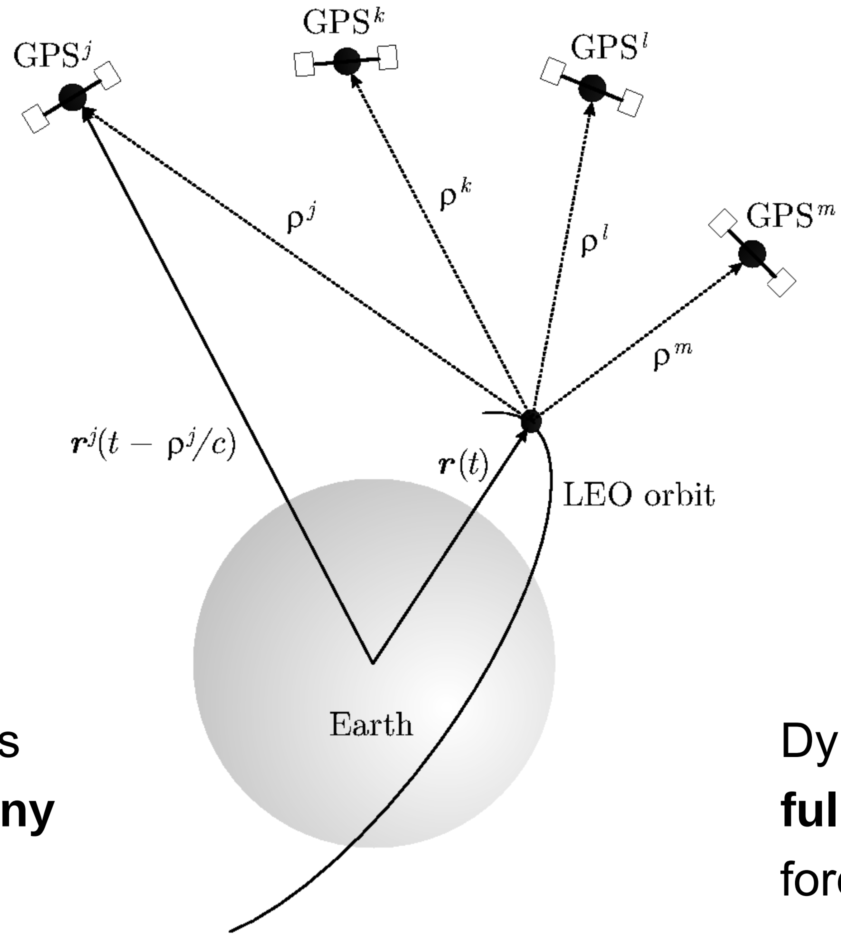

Dynamic orbit positions may be computed at **any epoch** within the arc

Dynamic positions are **fully dependent** on the force models used, e.g., on the gravity field model

Reduced-Dynamic Orbit Representation (1)

Equation of motion (in inertial frame) is given by:

$$\ddot{\boldsymbol{r}} = -GM\frac{\boldsymbol{r}}{r^3} + \boldsymbol{f}_1(t, \boldsymbol{r}, \dot{\boldsymbol{r}}, Q_1, ..., Q_d, P_1, ..., P_s)$$

$P_1, ..., P_s$ Pseudo-stochastic parameters

Pseudo-stochastic parameters are:

- additional empirical parameters characterized by a priori known **statistical properties**, e.g., by expectation values and a priori variances
- useful to **compensate** for deficiencies in dynamic models, e.g., deficiencies in models describing non-gravitational accelerations
- often set up as **piecewise constant accelerations** to ensure that satellite trajectories are continuous and differentiable at any epoch

Reduced-Dynamic Orbit Representation (2)

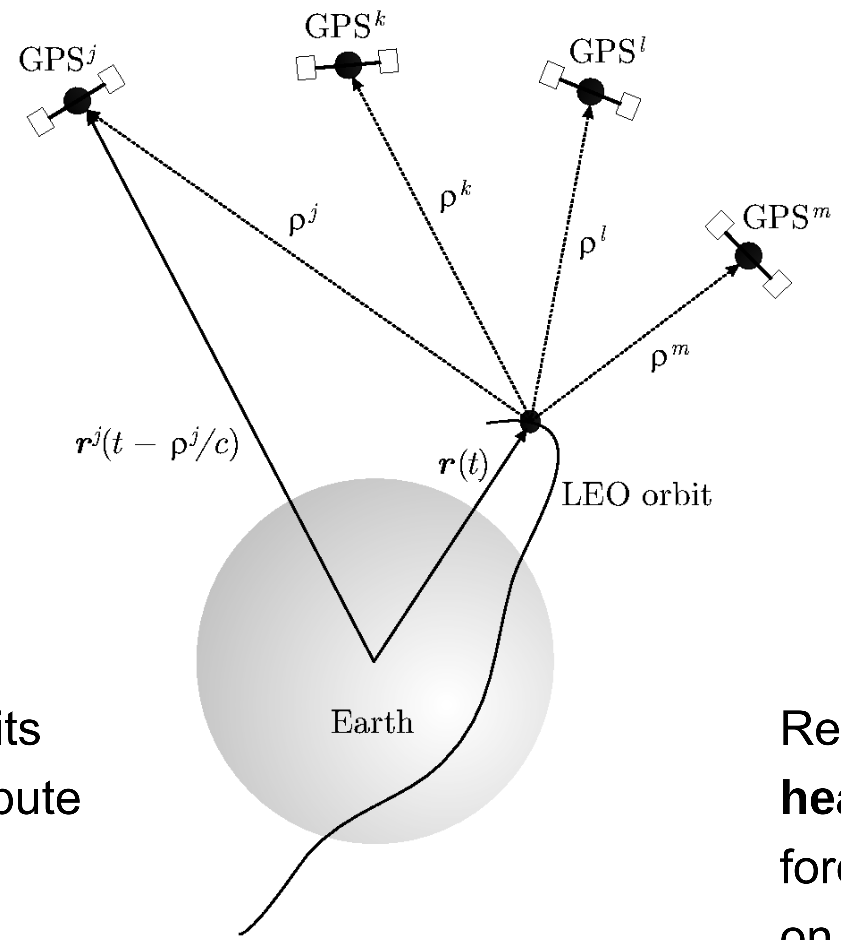

Reduced-dynamic orbits are well suited to compute LEO orbits of **highest quality**
(Jäggi et al., 2006; Jäggi, 2007)

Reduced-dynamic orbits **heavily depend** on the force models used, e.g., on the gravity field model
(Jäggi et al., 2008)

Partial Derivatives

Orbit improvement ($\boldsymbol{r}_0(t)$: numerically integrated **a priori orbit**):

$$\boldsymbol{r}(t) = \boldsymbol{r}_0(t) + \sum_{i=1}^{n} \frac{\partial \boldsymbol{r}_0}{\partial P_i}(t) \cdot (P_i - P_{0,i})$$

yields corrections to a priori parameter values $P_{0,i}$ by **least-squares**

Previously, for each parameter P_i the corresponding **variational equation**

$$\ddot{\boldsymbol{z}}_{P_i} = \boldsymbol{A}_0 \cdot \boldsymbol{z}_{P_i} + \boldsymbol{A}_1 \cdot \dot{\boldsymbol{z}}_{P_i} + \frac{\partial \boldsymbol{f}_1}{\partial P_i}$$

has to be solved to obtain the partials $\boldsymbol{z}_{P_i}(t) \doteq \dfrac{\partial \boldsymbol{r}_0}{\partial P_i}(t)$, e.g., by:

- Numerical integration for initial osculating elements
- Numerical quadrature for dynamic parameters
- Linear combinations for pseudo-stochastic parameters

(Jäggi, 2007)

Reduced-dynamic Orbit Representation (3)

Position epochs
(in GPS time)

Positions (km) &
Velocities (dm/s)
(Earth-fixed)

Clock corrections
are not provided

```
*  2009 11  2  0  0  0.00000000
PL15   -391.718353   6623.836682     79.317661 999999.999999
VL15  13710.157683   1908.731015 -77015.601314 999999.999999
*  2009 11  2  0  0 10.00000000
PL15   -377.980705   6625.284690      2.298385 999999.999999
VL15  13764.602016    987.250587 -77021.193676 999999.999999
*  2009 11  2  0  0 20.00000000
PL15   -364.190222   6625.811136    -74.721213 999999.999999
VL15  13815.825127     65.631014 -77016.232293 999999.999999
*  2009 11  2  0  0 30.00000000
PL15   -350.350131   6625.415949   -151.730567 999999.999999
VL15  13863.820409   -855.995477 -77000.719734 999999.999999
*  2009 11  2  0  0 40.00000000
PL15   -336.463660   6624.099187   -228.719134 999999.999999
VL15  13908.581905  -1777.497047 -76974.660058 999999.999999
*  2009 11  2  0  0 50.00000000
PL15   -322.534047   6621.861041   -305.676371 999999.999999
VL15  13950.104280  -2698.741871 -76938.058807 999999.999999
*  2009 11  2  0  1  0.00000000
PL15   -308.564533   6618.701833   -382.591743 999999.999999
VL15  13988.382807  -3619.598277 -76890.923043 999999.999999
```

Excerpt of reduced-dynamic GOCE positions at begin of 2 Nov, 2009

GO_CONS_SST_PRD_2__20091101T235945_20091102T235944_0001

GOCE Sensor Offsets (1)

Phase center offsets $\delta \boldsymbol{r}_{leo,ant}$:

- are needed in the inertial or Earth-fixed frame and have to be transformed from the satellite frame using **attitude data** from the star-trackers

- consist of a frequency-independent **instrument offset**, e.g., defined by the center of the instrument‘s mounting plane (CMP) in the satellite frame

- consist of frequency-dependent **phase center offsets** (PCOs), e.g., defined wrt the center of the instrument‘s mounting plane in the antenna frame (ARF)

- consist of frequency-dependent **phase center variations** (PCVs) varying with the direction of the incoming signal, e.g., defined wrt the PCOs in the antenna frame

GOCE Sensor Offsets (2)

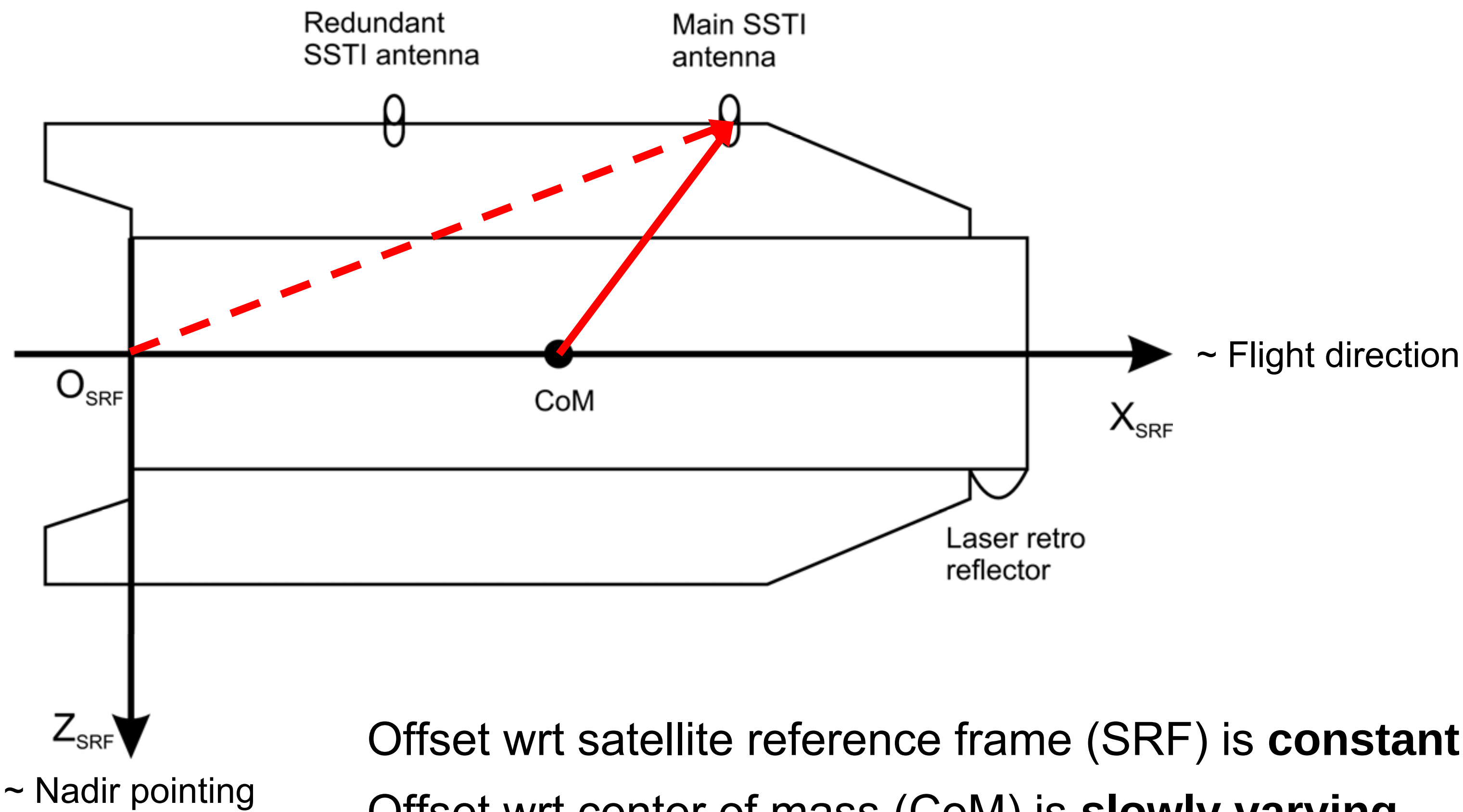

Offset wrt satellite reference frame (SRF) is **constant**

Offset wrt center of mass (CoM) is **slowly varying**

GOCE Sensor Offsets (3)

Table 1: CoM coordinates in SRF system

CoM	X_{SRF}[m]	Y_{SRF}[m]	Z_{SRF}[m]
Begin of Life (BoL)	2.4990	0.0036	0.0011
End of Life (EoL)	2.5290	0.0038	0.0012

Table 2: SSTI antenna CMP coordinates in SRF system

CMP coordinates	X_{SRF} [m]	Y_{SRF}[m]	Z_{SRF}[m]
Main	3.1930	0.0000	-1.0922
Redundant	1.3450	0.0000	-1.0903

Table 3: SSTI antenna CMP coordinates wrt to CoM (BoL)

CMP coordinates	X_{CoM} [m]	Y_{CoM}[m]	Z_{CoM}[m]
Main	0.6940	-0.0036	-1.0933
Redundant	-1.1540	-0.0036	-1.0914

Table 4: SSTI antenna phase center offsets in ARF system

Phase center offsets	X_{ARF}[mm]	Y_{ARF}[mm]	Z_{ARF}[mm]
Main: L1	-0.18	3.51	-81.11
Main: L2	-1.22	-1.00	-84.18
Redundant: L1	-0.96	3.14	-81.33
Redundant: L2	-1.48	-1.20	-84.18

Derived from Bigazzi and Frommknecht (2010)

GOCE GPS Antenna

L1, L2, Lc phase center offsets

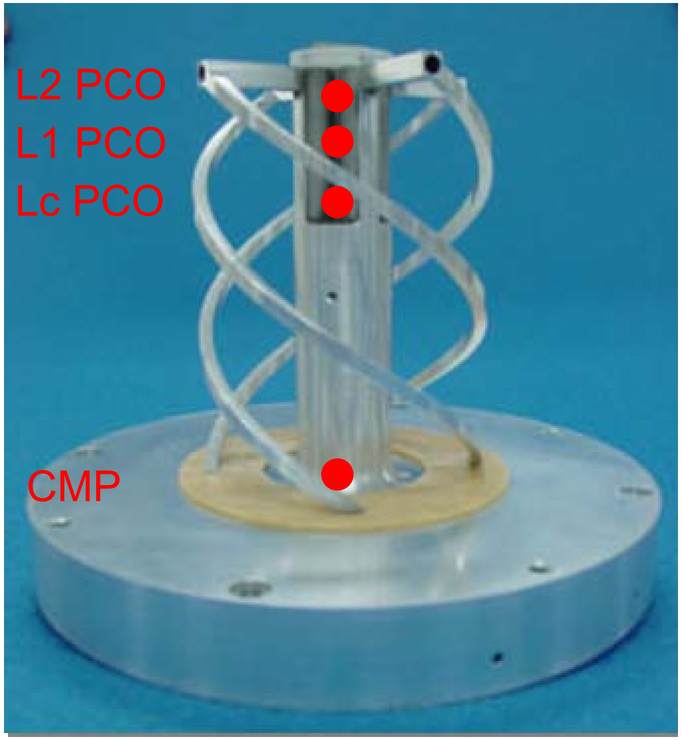

Measured from ground calibration in anechoic chamber

Lc phase center variations

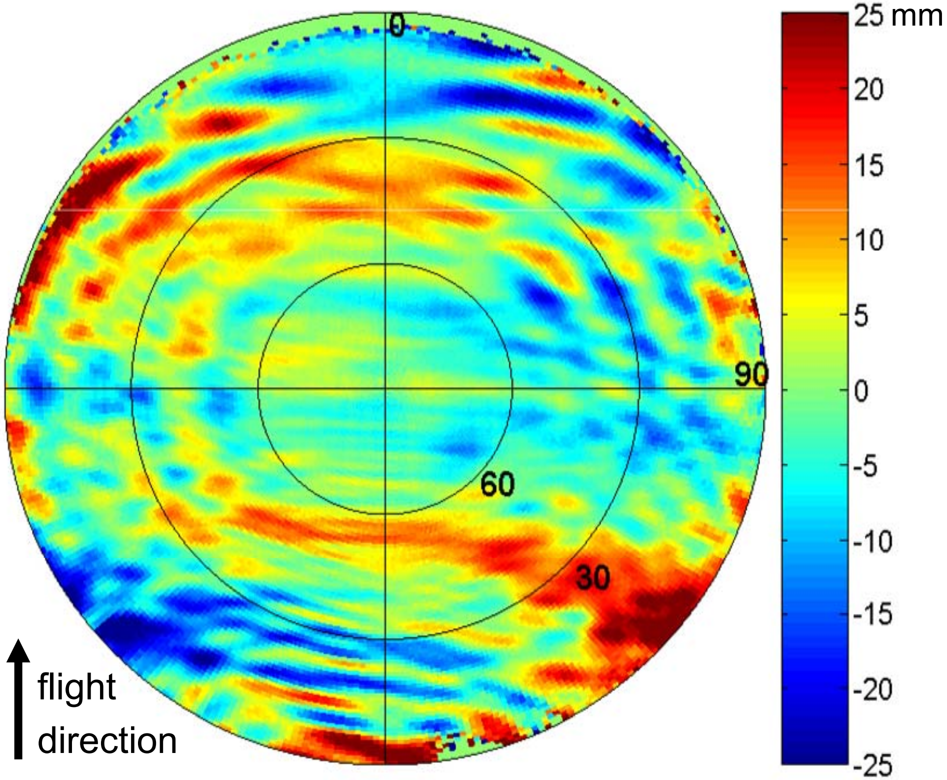

Empirically derived during orbit determination according to Jäggi et al. (2009b)

GOCE High-level Processing Facility: Orbit Groups

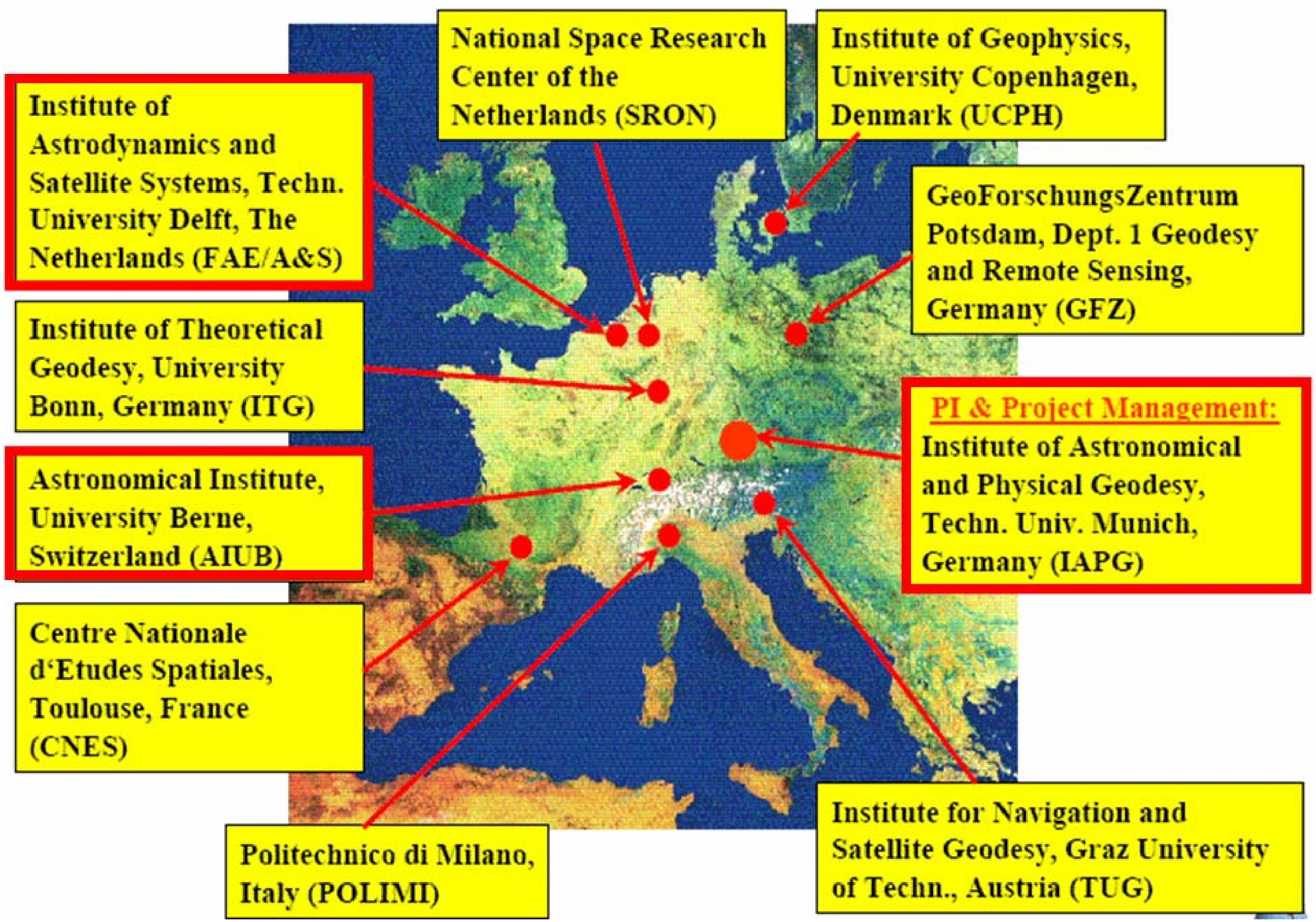

Responsibilities:

DEOS => **RSO**
(Rapid Science Orbit)

AIUB => **PSO**
(Precise Science Orbit)

IAPG => Validation

GOCE High-level Processing Facility: Orbit Products

	Orbit solution	Software	GPS Observ.	GPS products	Sampling	Data batches	Latency
RSO	reduced-dynamic	GEODYN	triple-diff	IGS rapid	10 sec	30 h	1 day
	kinematic	GHOST	zero-diff	CODE rapid	1 sec	24 h	1 day
PSO	reduced-dynamic	BERNESE	zero-diff	CODE final	10 sec	30 h	7-10 days
	kinematic	BERNESE	zero-diff	CODE final	1 sec	30 h	7-10 days

(Visser et al., 2009)

Accuracy requirement: 2 cm

(Bock et al., 2007)

SST_PSO_2 Product

The final Level-2 PSO product consists of:

SST_PKI_2: Kinematic positions, 1 sec, SP3c format

SST_PRD_2: Reduced-dynamic positions and velocities, 10 sec, SP3c format

SST_PRM_2: Rotation from Earth-fixed to inertial frame, 1 sec, quaternions

SST_PCV_2: Covariance matrix of kinematic positions, 4 off-diagonal blocks

SST_PRP_2: Report, PDF format

The data files cover a time span of 24h

(GOCE Level 2 Product Data Handbook, 2009)

GPS Data Availability

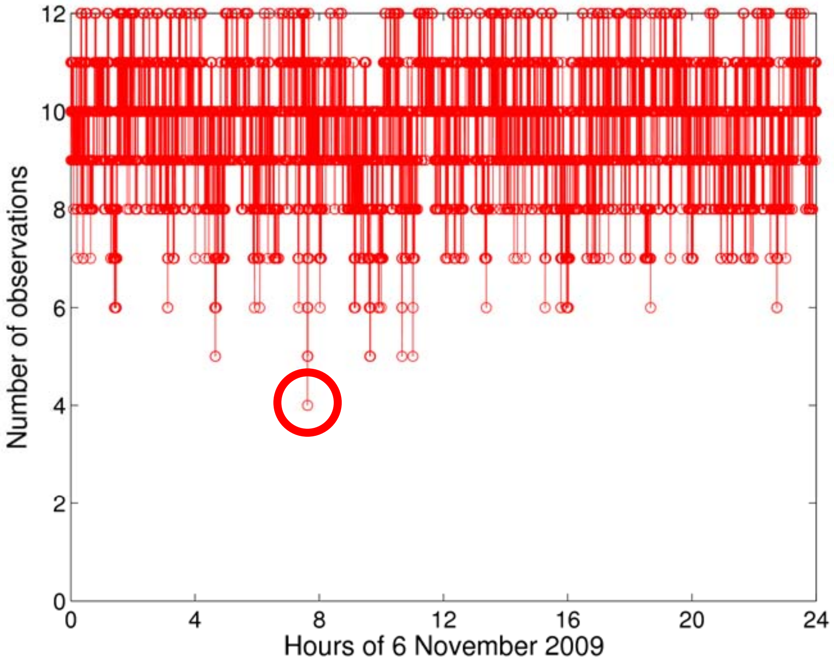

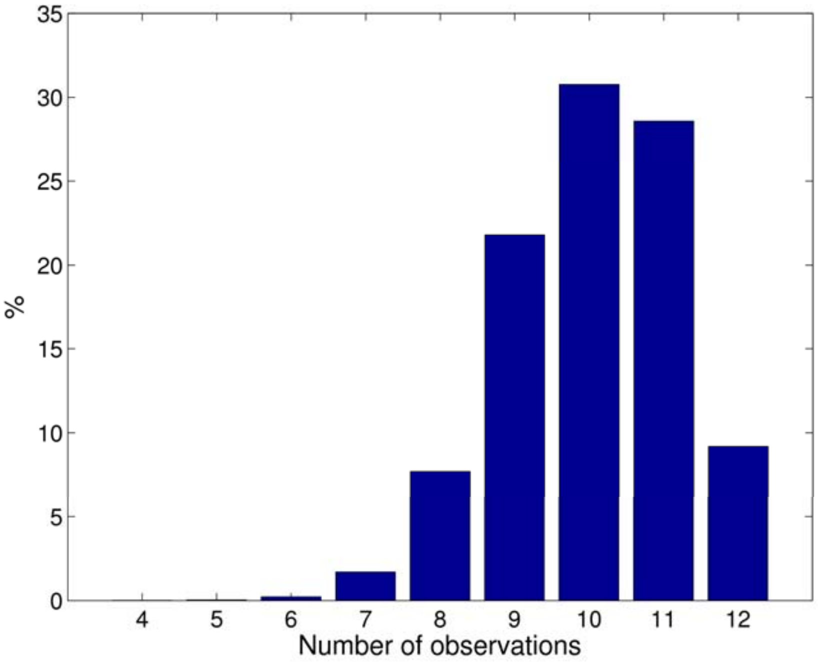

GPS data availability is excellent:

- **12 channel** GPS receiver provides 1Hz data with hardly any gaps; less than 5 satellites are tracked for **less than 0.2%** of all measurement epochs

→ Missing kinematic positions: **about 0.5%**

Visualization of GOCE PSO Product

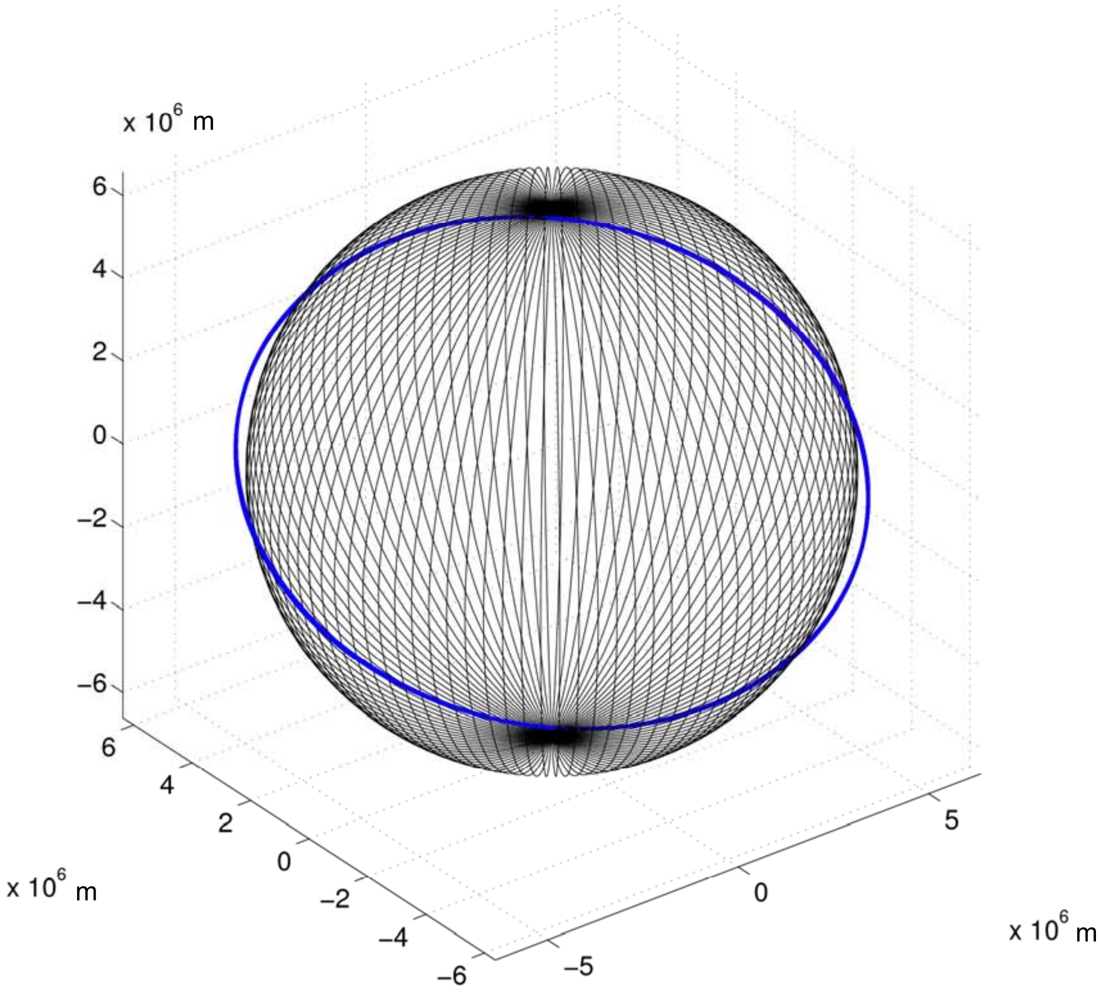

It is more instructive to look at differences between orbits in well suited coordinate systems …

Co-Rotating Orbital Frames

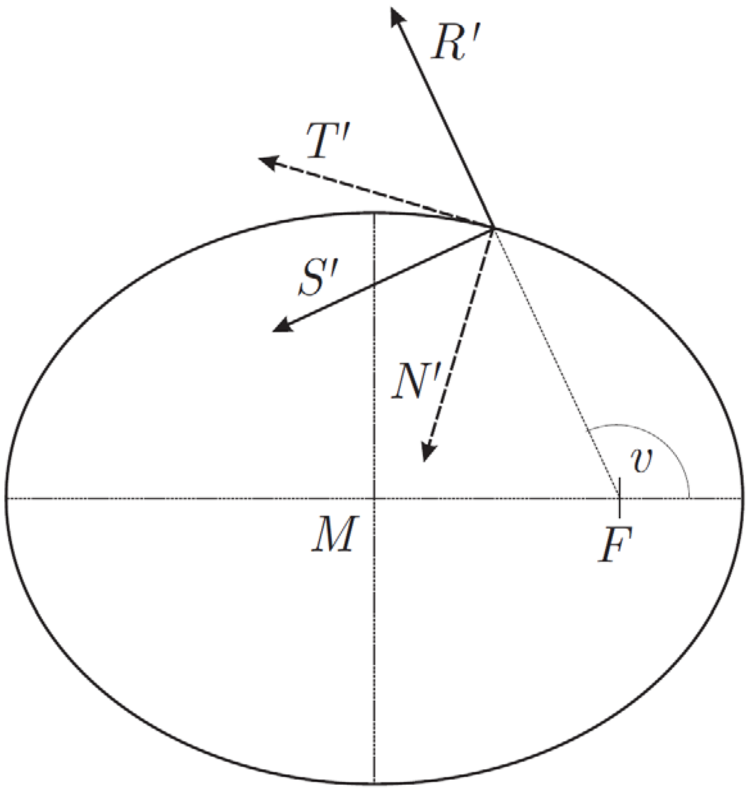

R, S, C unit vectors are pointing:
- into the radial direction
- normal to **R** in the orbital plane
- normal to the orbital plane (cross-track)

T, N, C unit vectors are pointing:
- into the tangential (along-track) direction
- normal to **T** in the orbital plane
- normal to the orbital plane (cross-track)

Small eccentricities: **S~T** (velocity direction)

Orbit Differences KIN-RD (Begin of Mission)

Differences at epochs of kin. positions

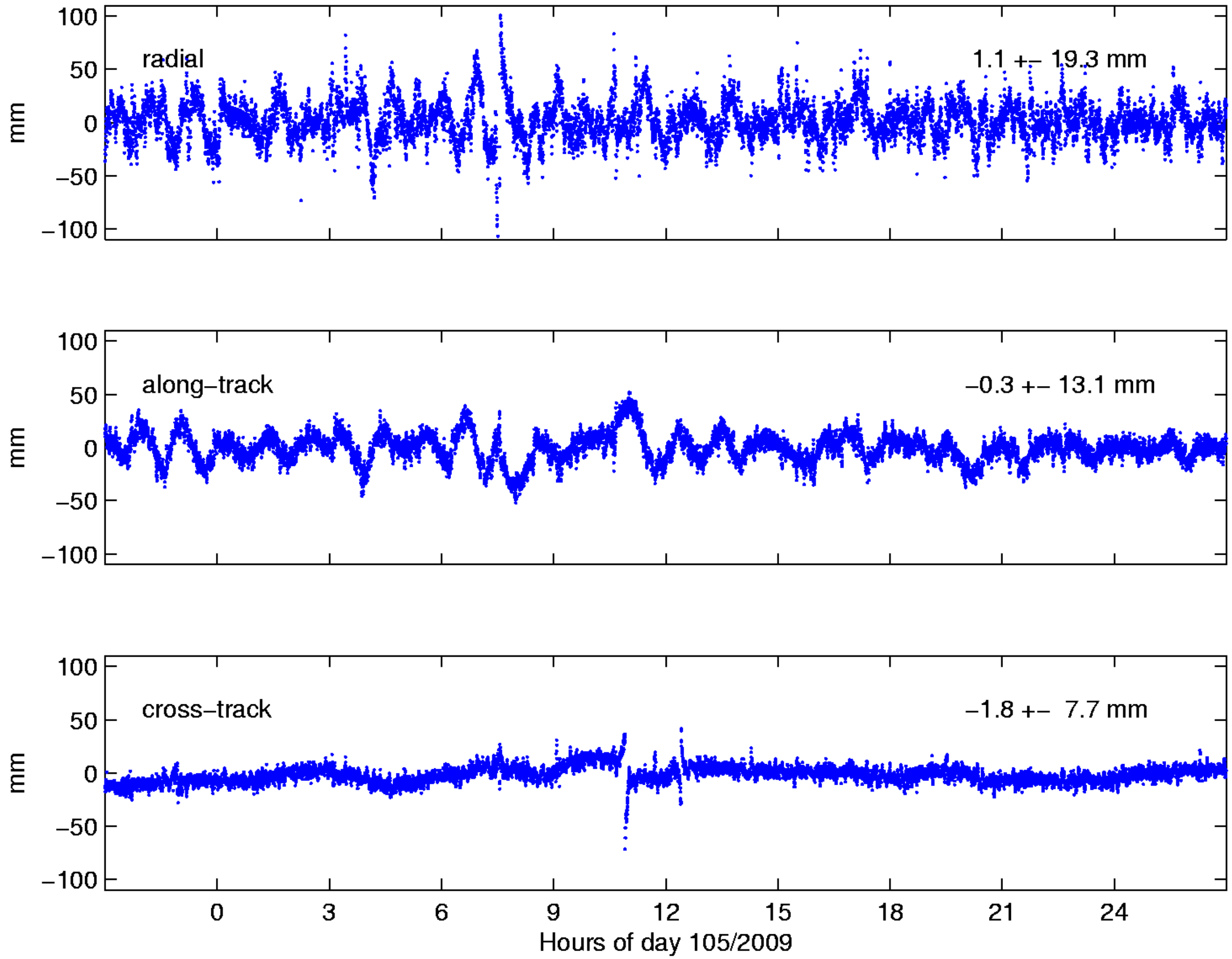

Orbit Differences KIN-RD, Time-Differenced

Largest scatter of kin. positions

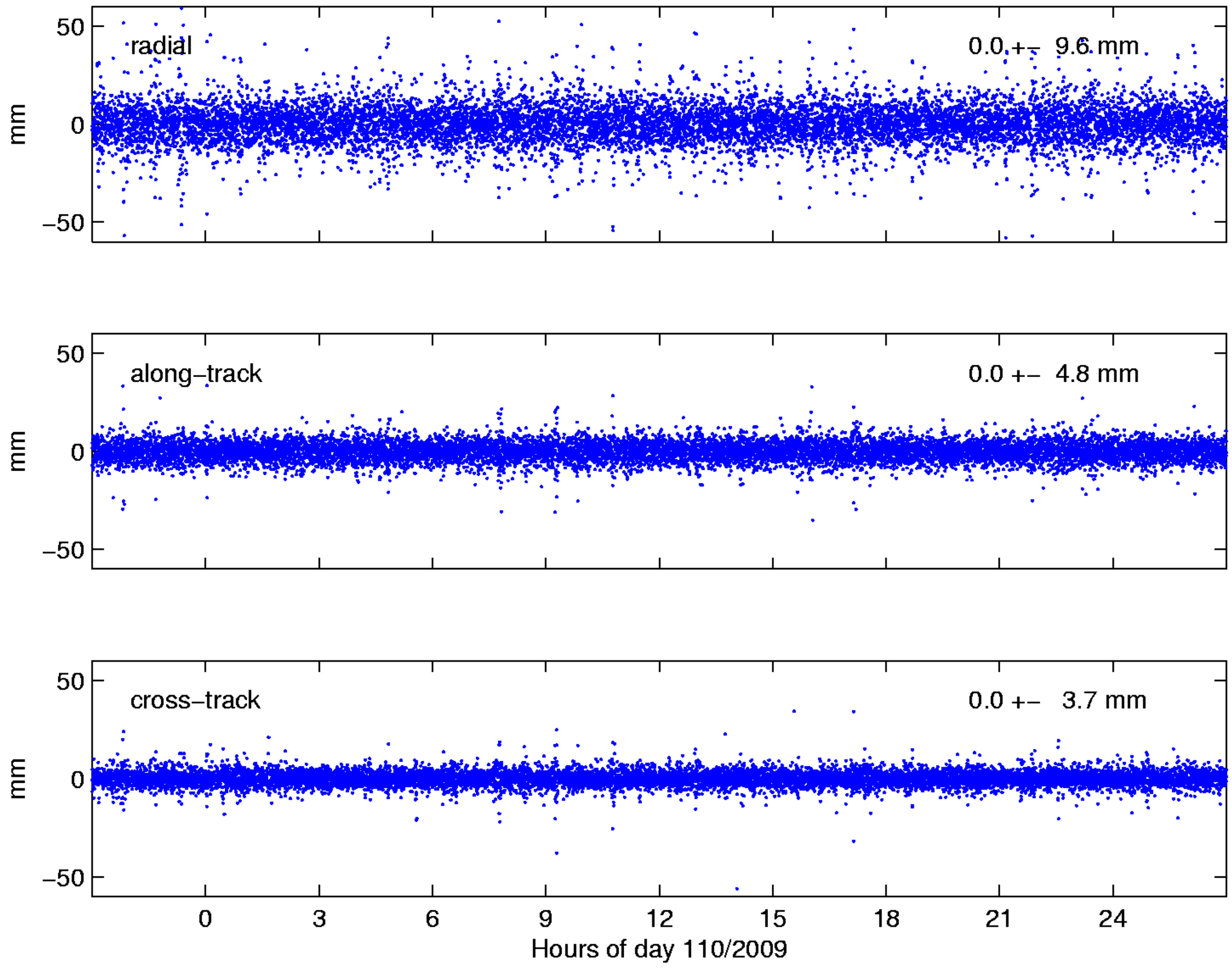

Pseudo-Stochastic Accelerations (Begin of Mission)

First drag-free flight on 7 May

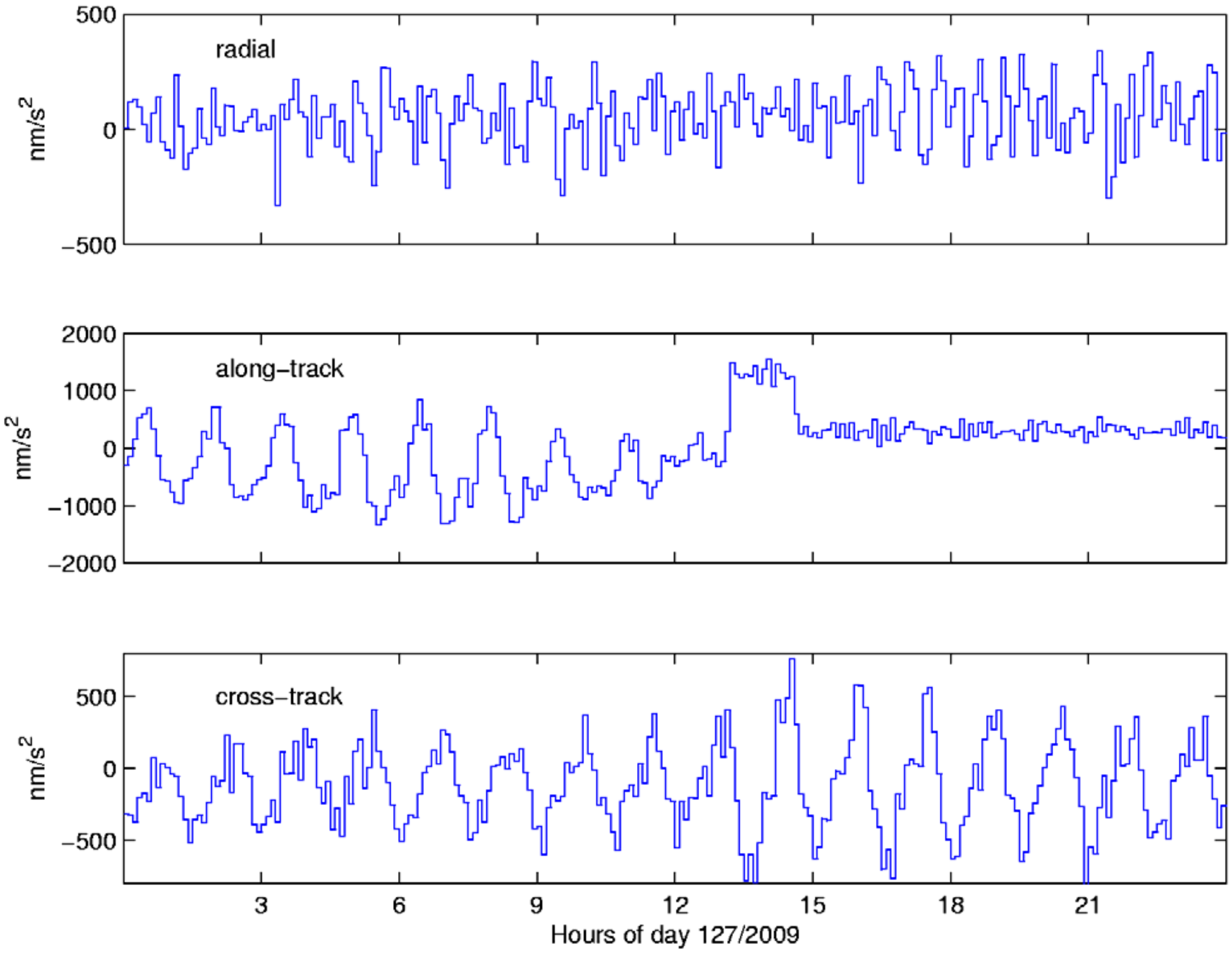

Improving GOCE Orbit Determination (1)

PCV modeling is one of the limiting factors for most precise LEO orbit determination. Unmodeled PCVs are systematic errors, which

- **directly** propagate into kinematic orbit determination and severly degrade the position estimates

- propagate into reduced-dynamic orbit determination to a smaller, **but still large extent**

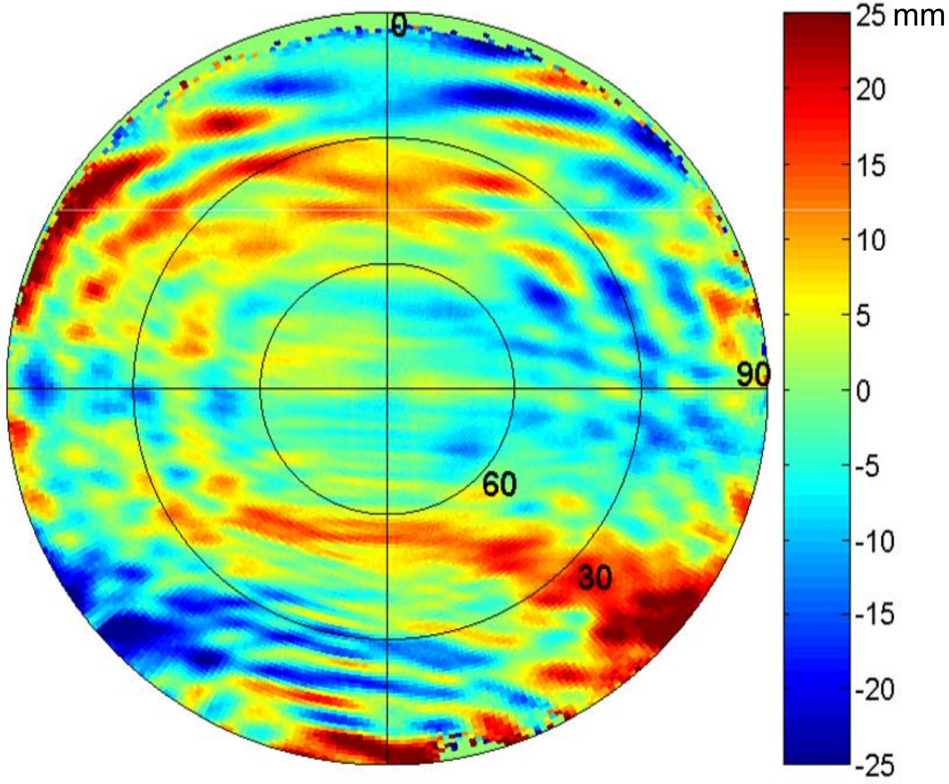

Improving GOCE Orbit Determination (2)

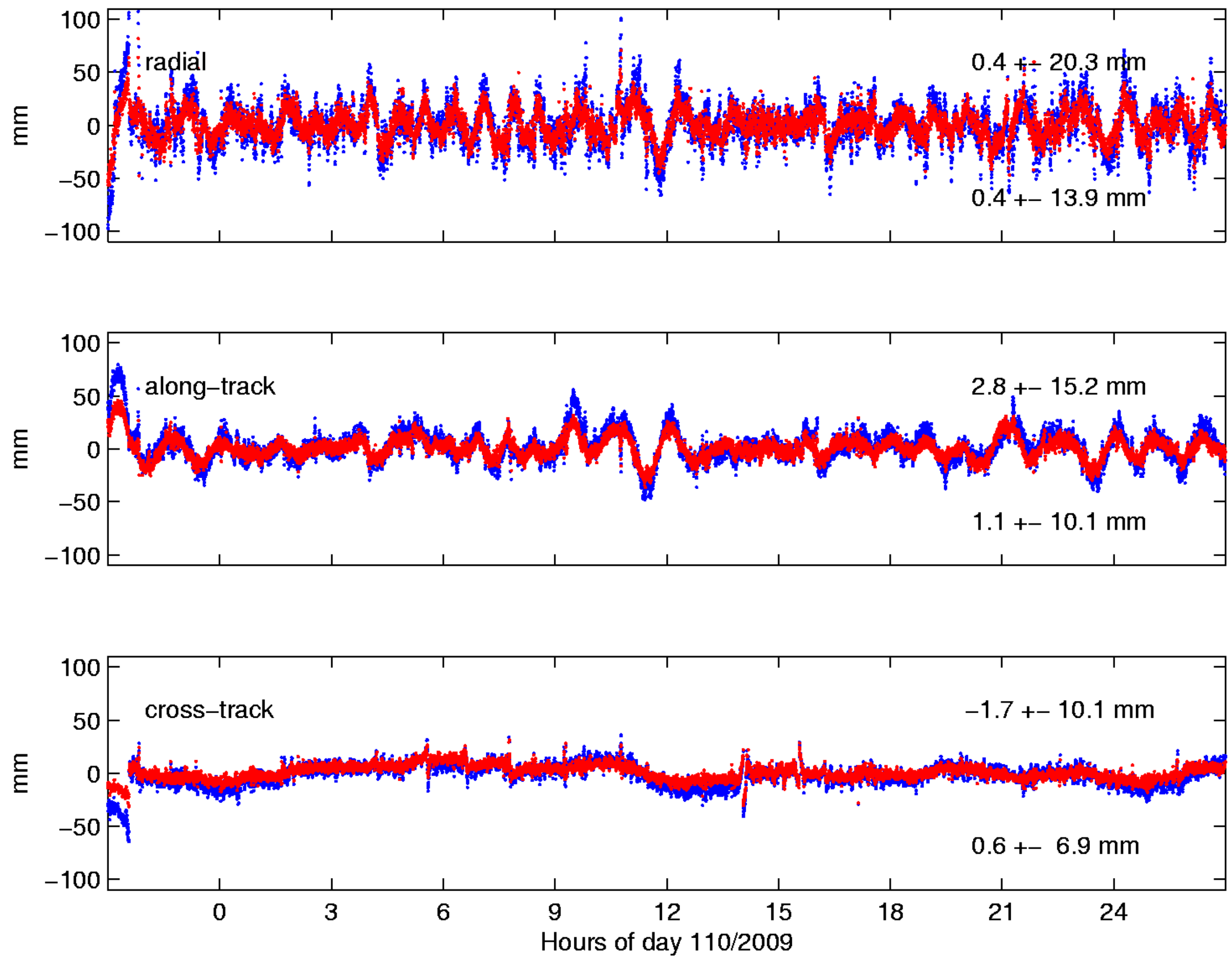

w/o PCV

with PCV

Orbit Differences KIN-RD

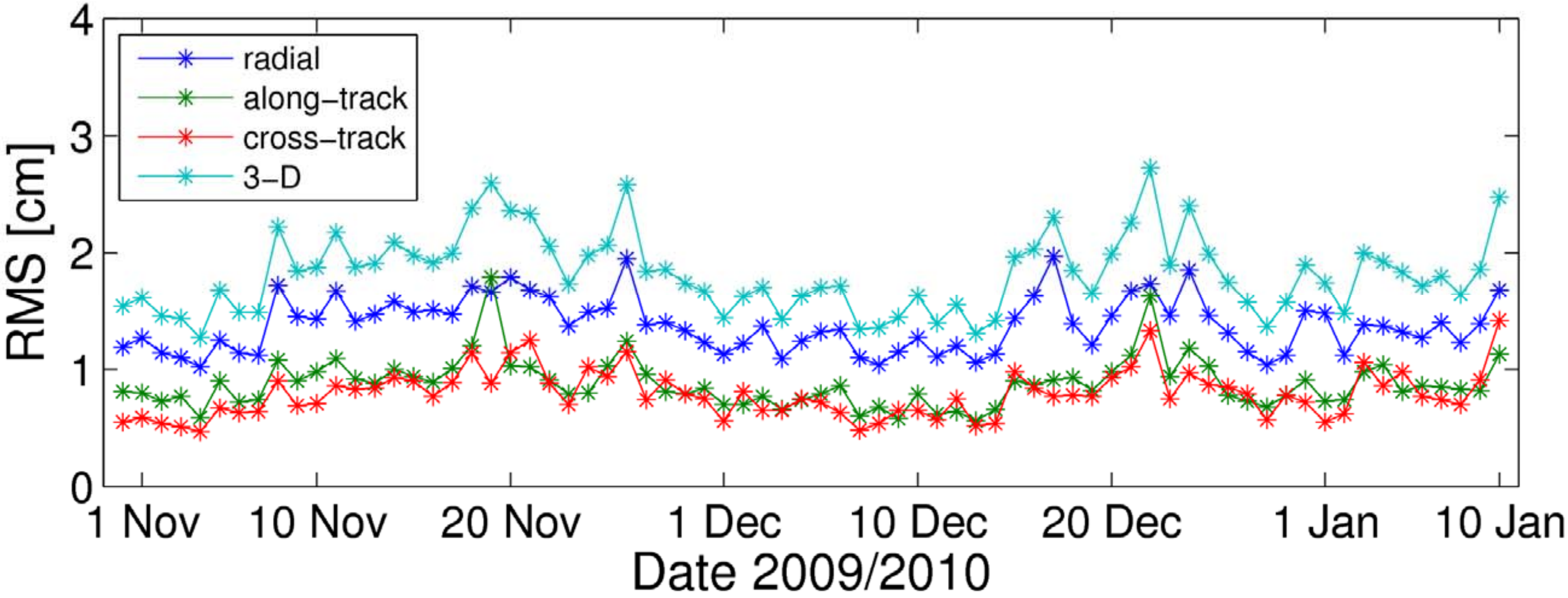

Remark on KIN-RD differences:

The differences show the **consistency** between both orbits and give an impression of the quality of kinematic positions, but they are **not** an indicator for orbit accuracy

GOCE Orbit Validation by Satellite Laser Ranging (SLR)

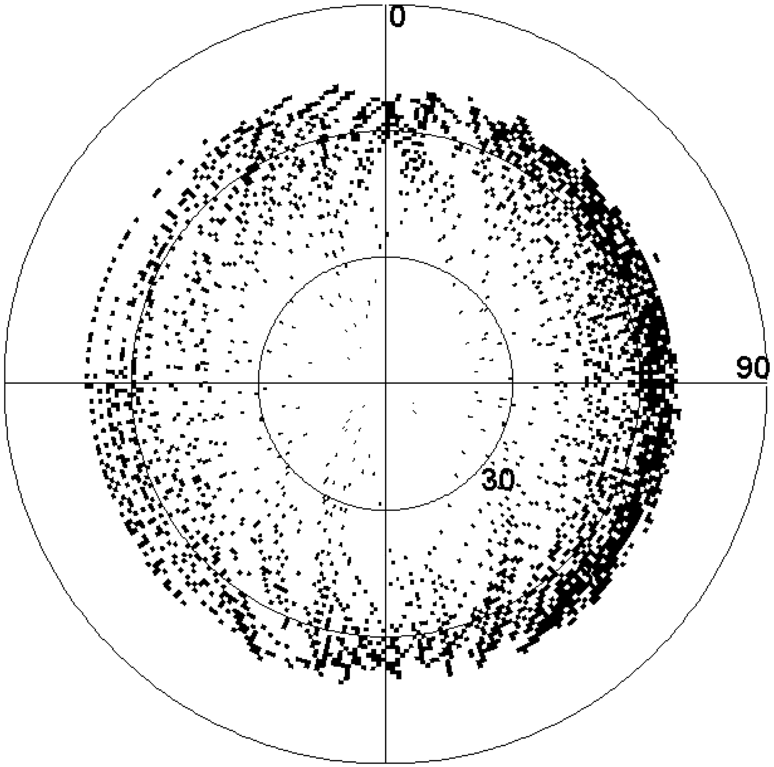

Distribution of SLR measurements as seen from the GOCE satellite (mission beginning)

GOCE Orbit Accuracy from SLR Residuals (1)

LEO orbits may be shifted up to several cm's in the cross-track direction by unmodeled PCVs.

Thanks to the low orbital altitude of GOCE it could be confirmed for the first time with SLR data that the PCV-induced cross-track shifts are real (see measurements from the SLR stations in the east and west directions at low elevations).

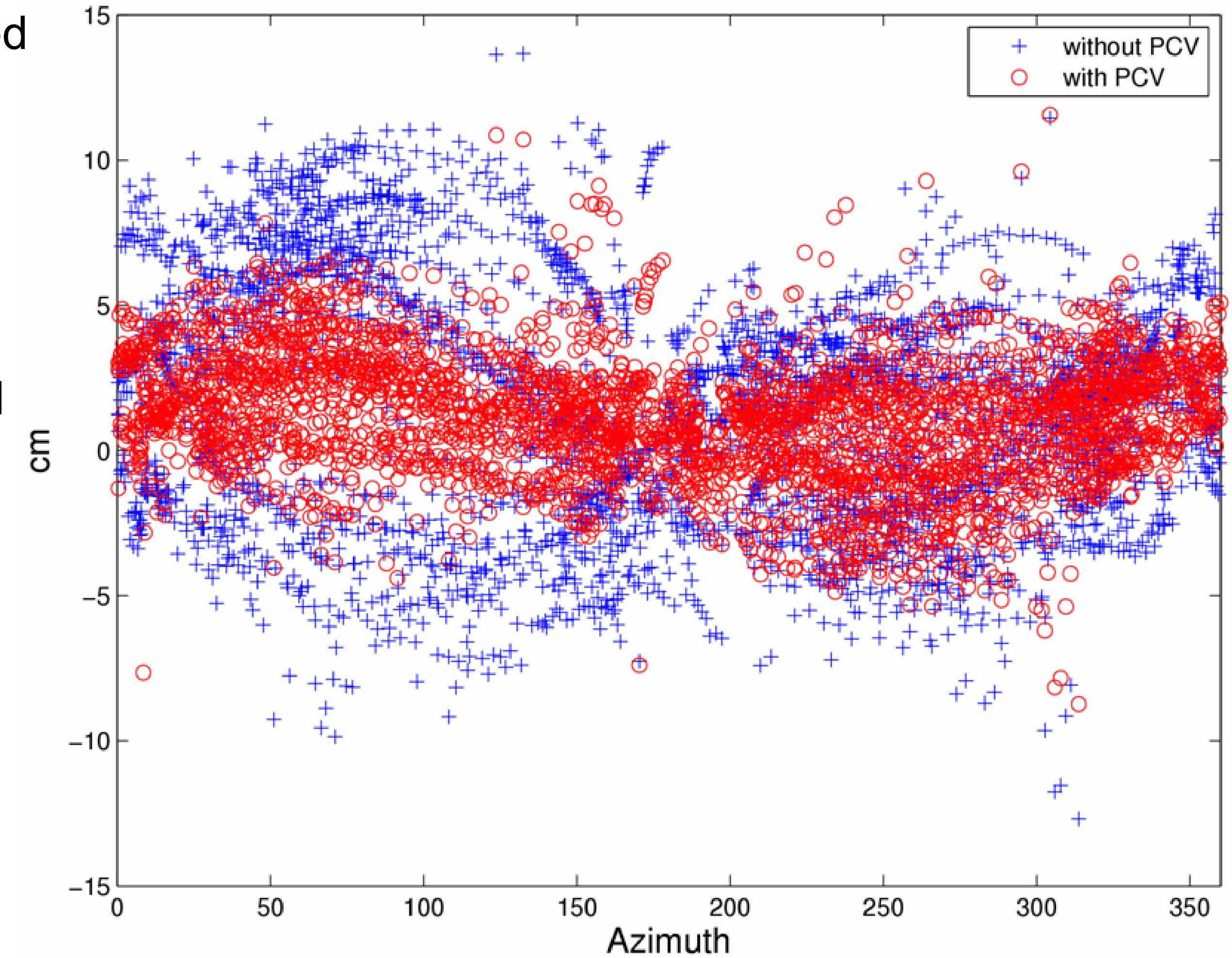

GOCE Orbit Accuracy from SLR Residuals (2)

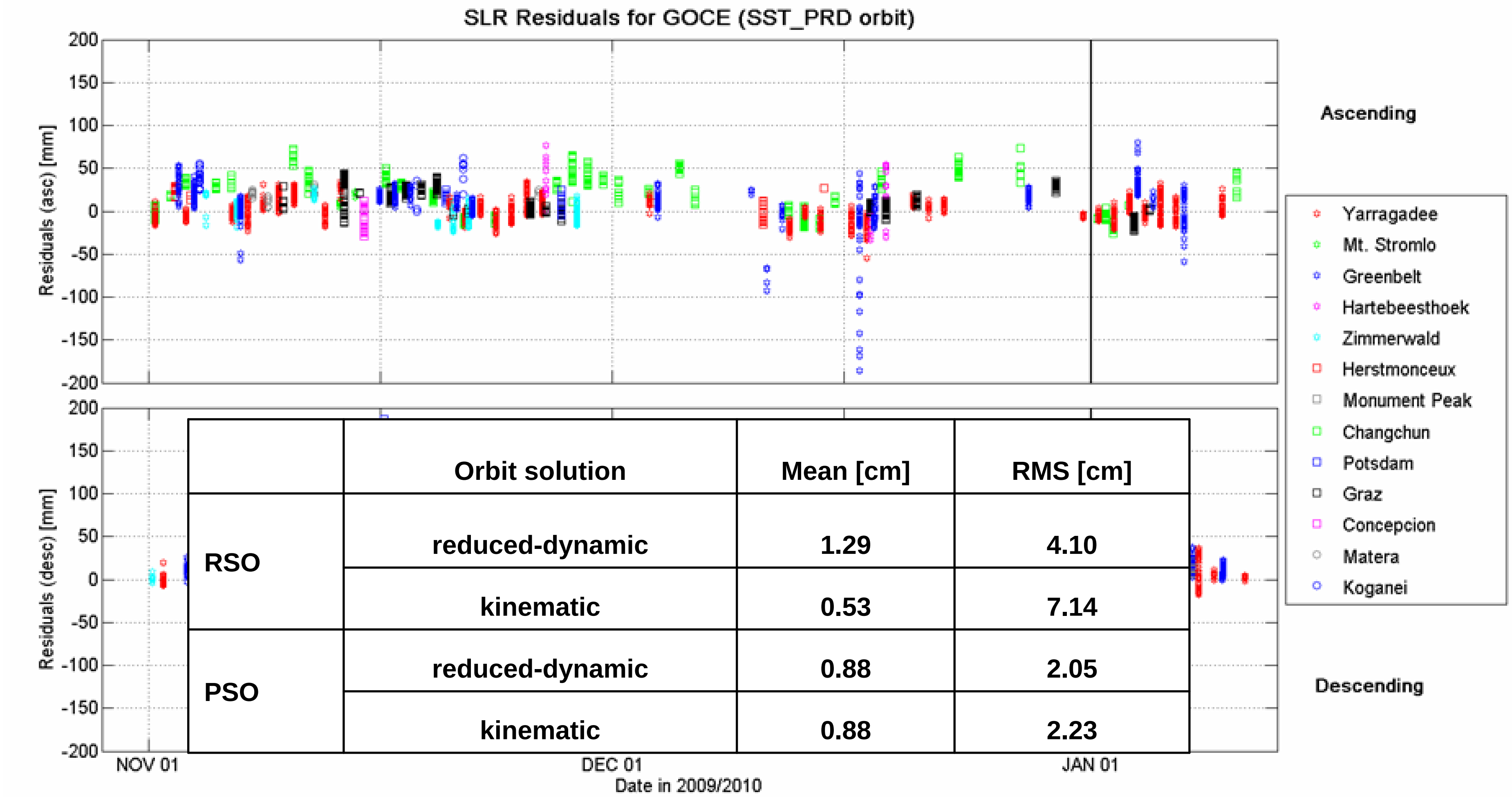

	Orbit solution	Mean [cm]	RMS [cm]
RSO	reduced-dynamic	1.29	4.10
	kinematic	0.53	7.14
PSO	reduced-dynamic	0.88	2.05
	kinematic	0.88	2.23

Orbit Differences KIN-RD on 2 Nov, 2009 (1)

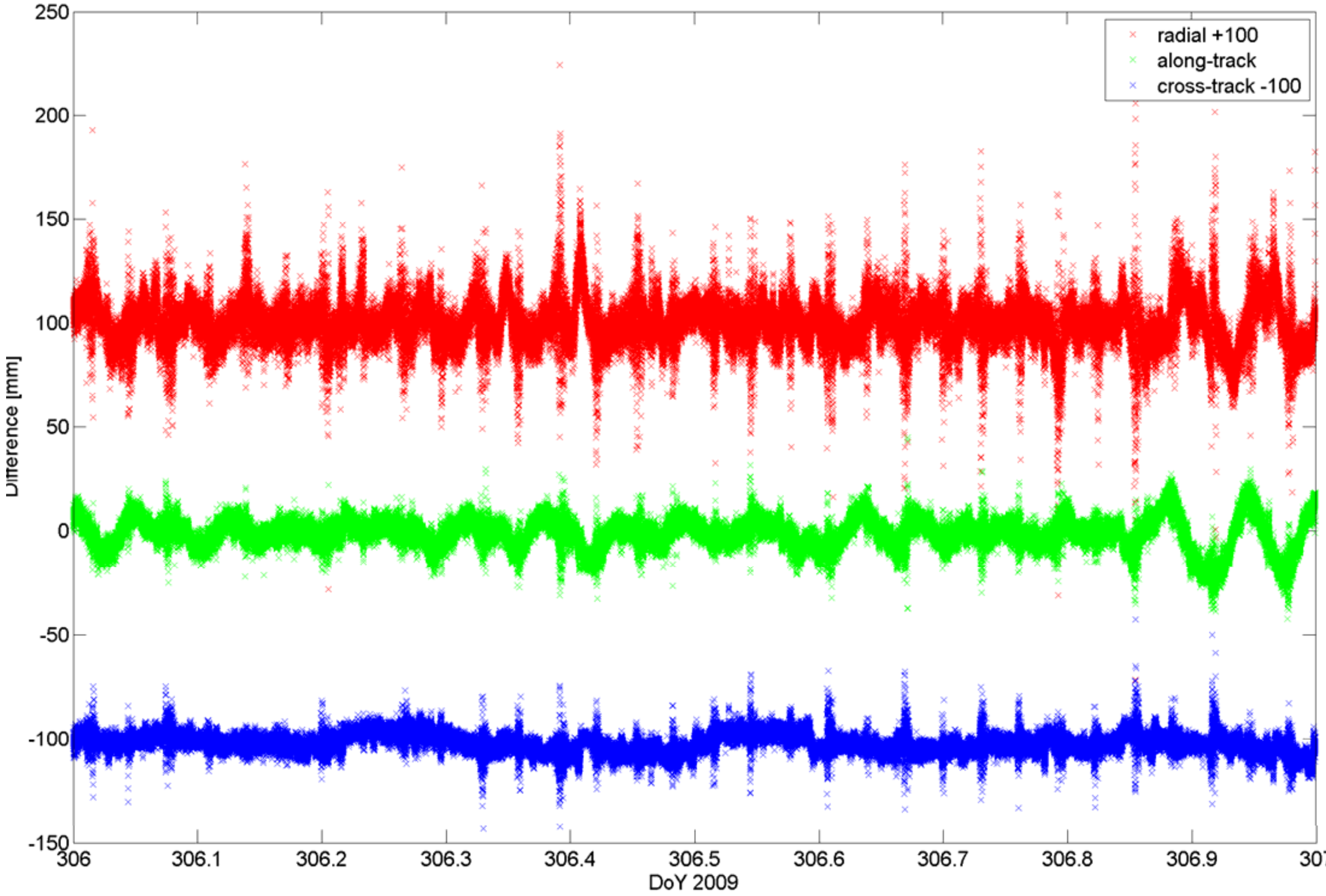

Orbit Differences KIN-RD on 2 Nov, 2009 (2)

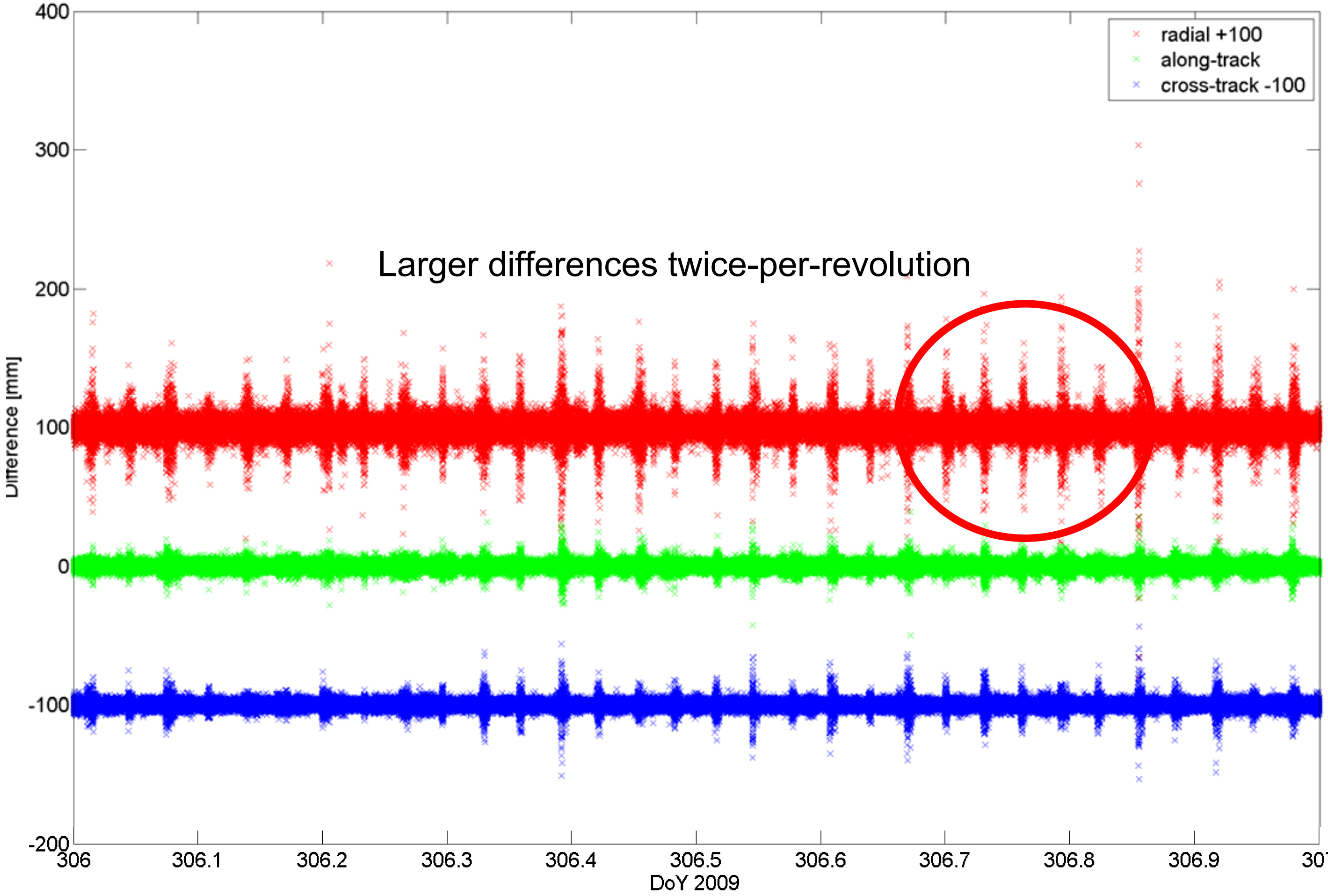

Orbit Differences KIN-RD on 2 Nov, 2009 (3)

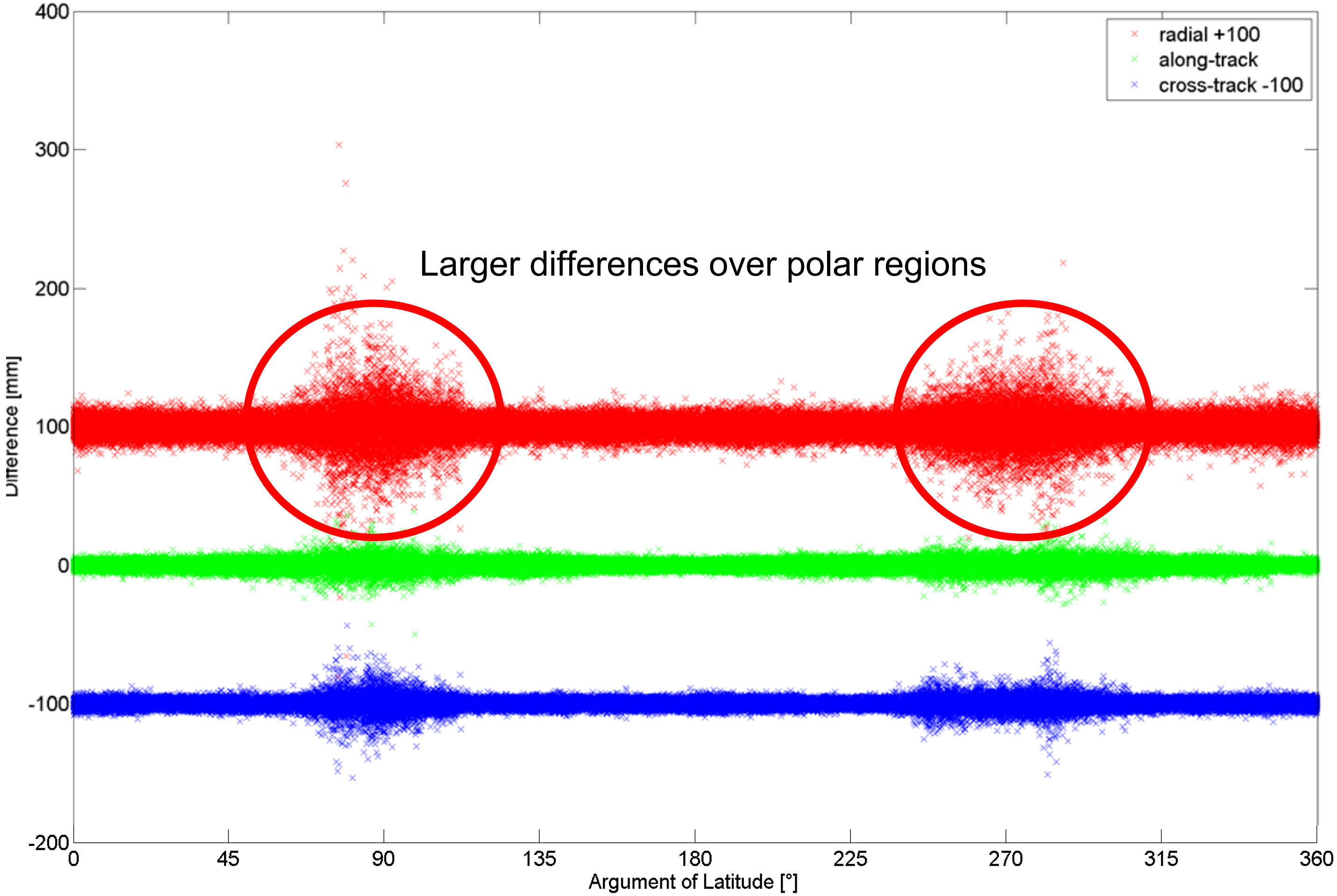

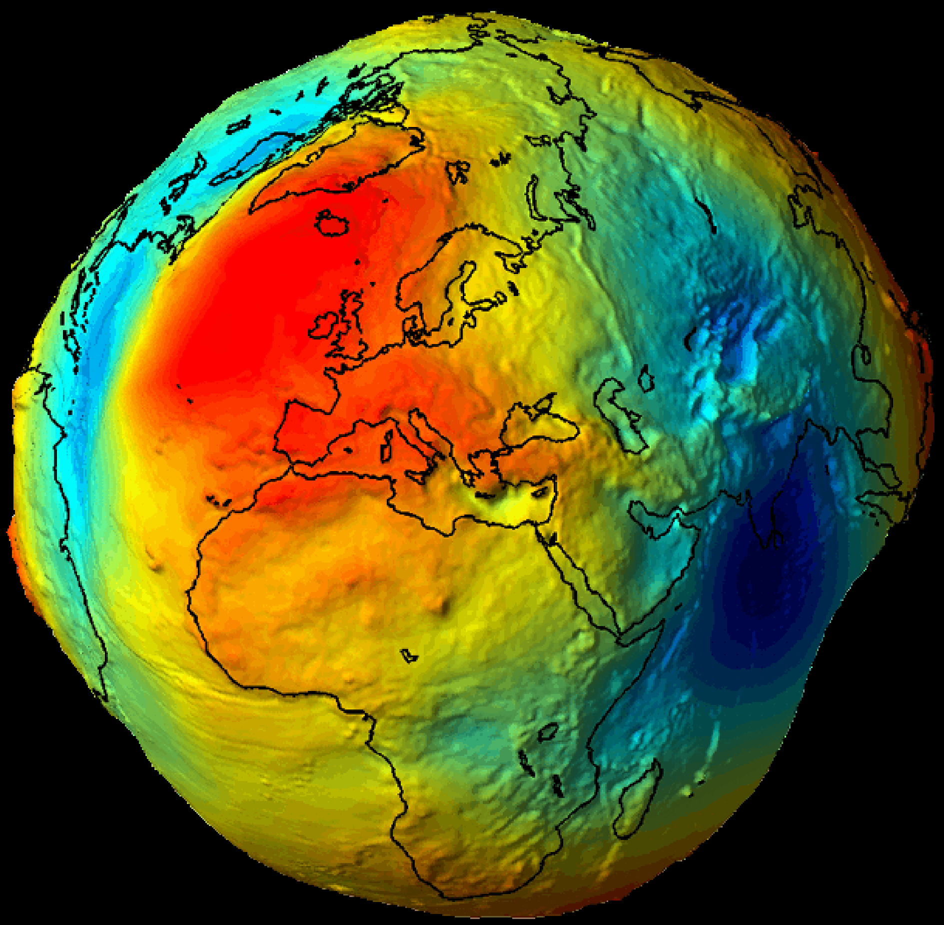

GPS-only Gravity Field Recovery

Kinematic Orbit Positions
Pseudo-Observations with Covariance Information

Accelerometer Data
(optional)

Set-Up of an Orbit Determination Problem by Least-Squares
- computation of the observation equations for each daily arc by numerical integration
  (estimated parameters: SH coefficients, arc-specific parameters, e.g., initial conditions and pulses)
- construction of the normal equations for each daily arc

Manipulation of Normal Equation Systems
- manipulation and subsequent pre-elimination of arc-specific parameters
  (e.g., constraining or downsampling of pulses)
- accumulation of daily normal equations into weekly, monthly, and annual systems
- regularization of SH coefficients
  (not used)
- inversion of the resulting normal equation systems

(Jäggi et al., 2009a)

GOCE GPS-only Solutions (1)

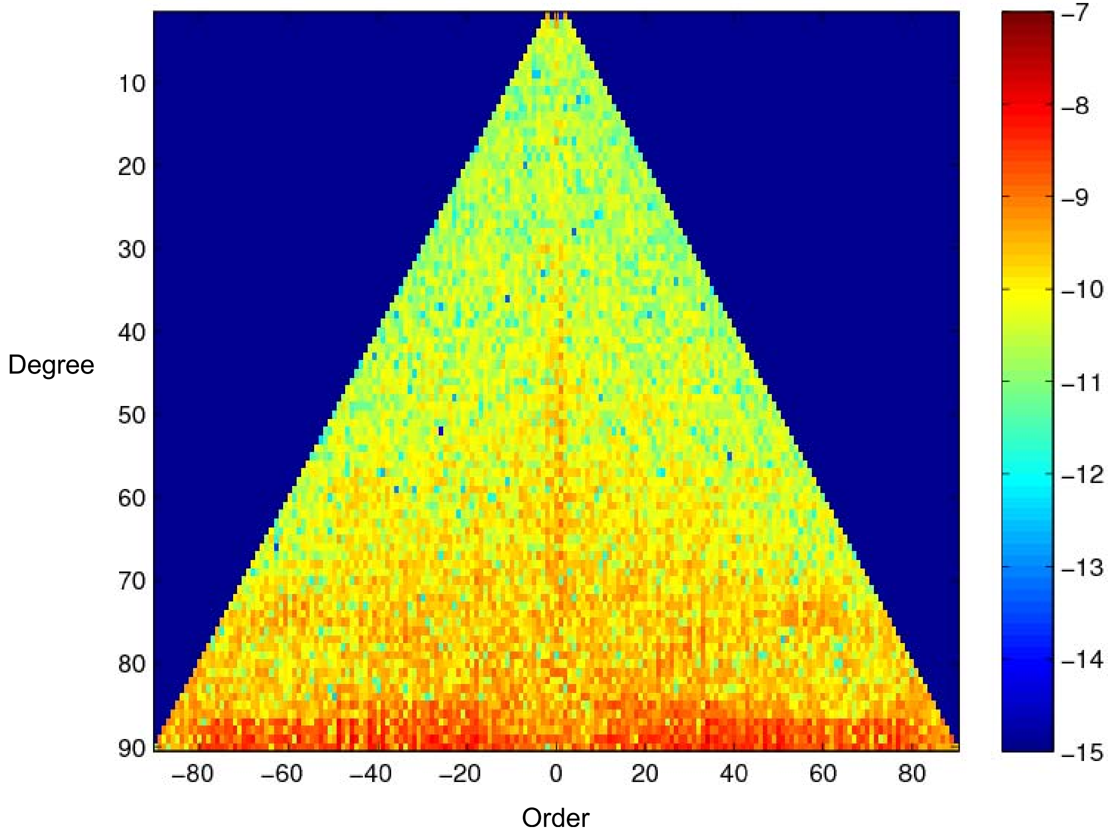

Reference field:

ITG-GRACE03S

Differences:

0.7-years GOCE

Difference degree amplitudes $\delta d_i \doteq \sqrt{\sum_{m=0}^{i} \left(\Delta\bar{C}_{i,m}^2 + \Delta\bar{S}_{i,m}^2 \right)}$ are often used for comparisons

GOCE GPS-only Solutions (2)

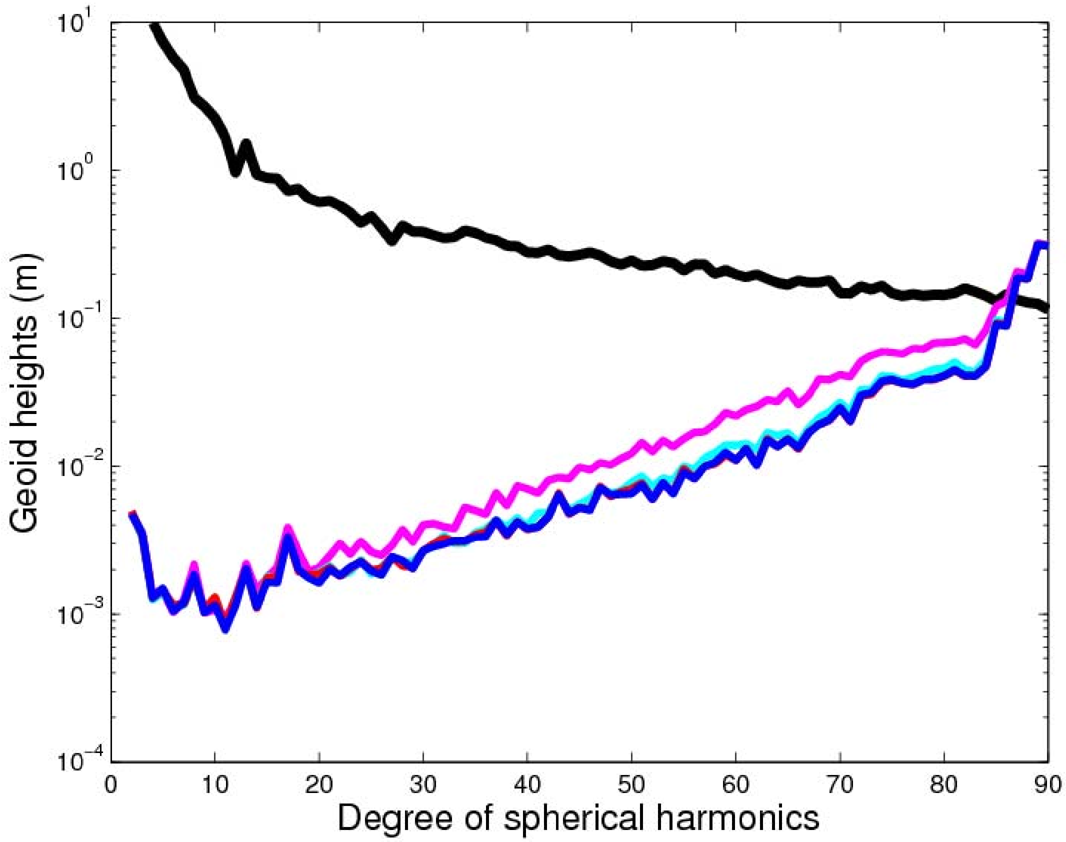

Reference field:

ITG-GRACE03S

Differences:

30-sec positions

5-sec positions

1-sec positions

1-sec pos. + cov.

Kinematic positions should be used with at least 5-sec sampling for GOCE gravity field recovery

Comparison of different GPS-only Solutions

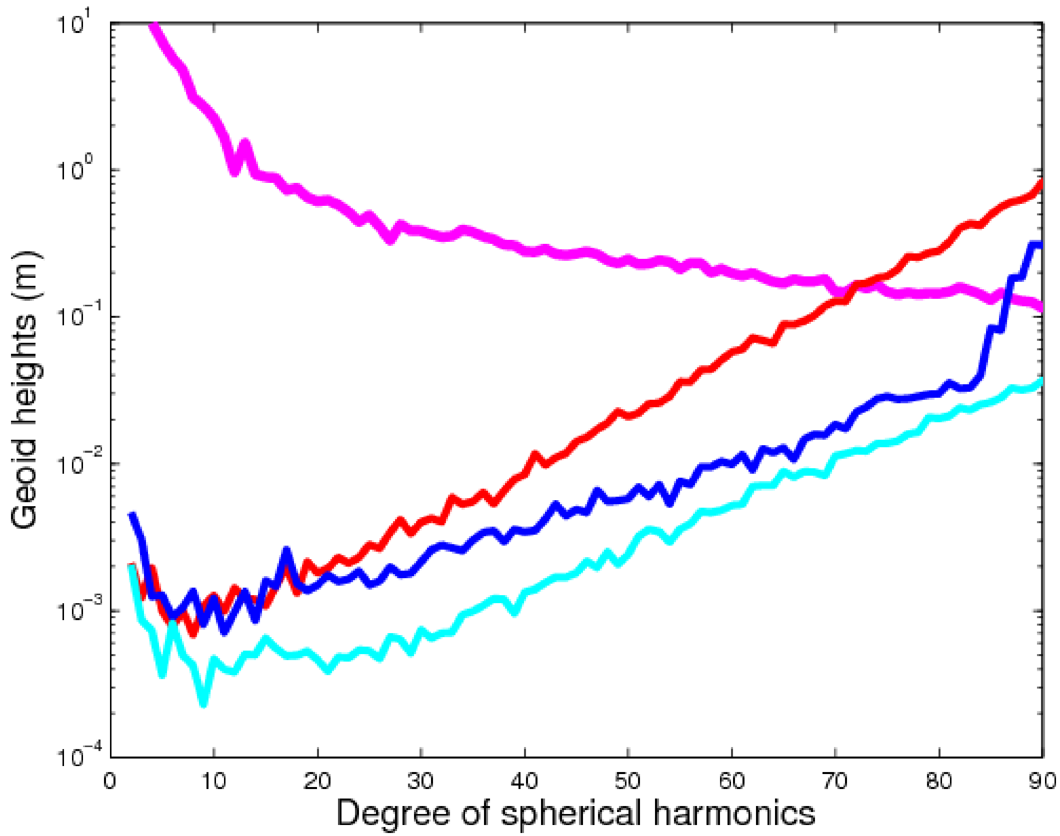

Reference field:

ITG-GRACE03S

Differences:

1-year GRACE

0.7-years GOCE

8-years CHAMP

Low orbital altitude of GOCE significantly improves the slope of the difference degree amplitudes

Impact of the Polar Gap (1)

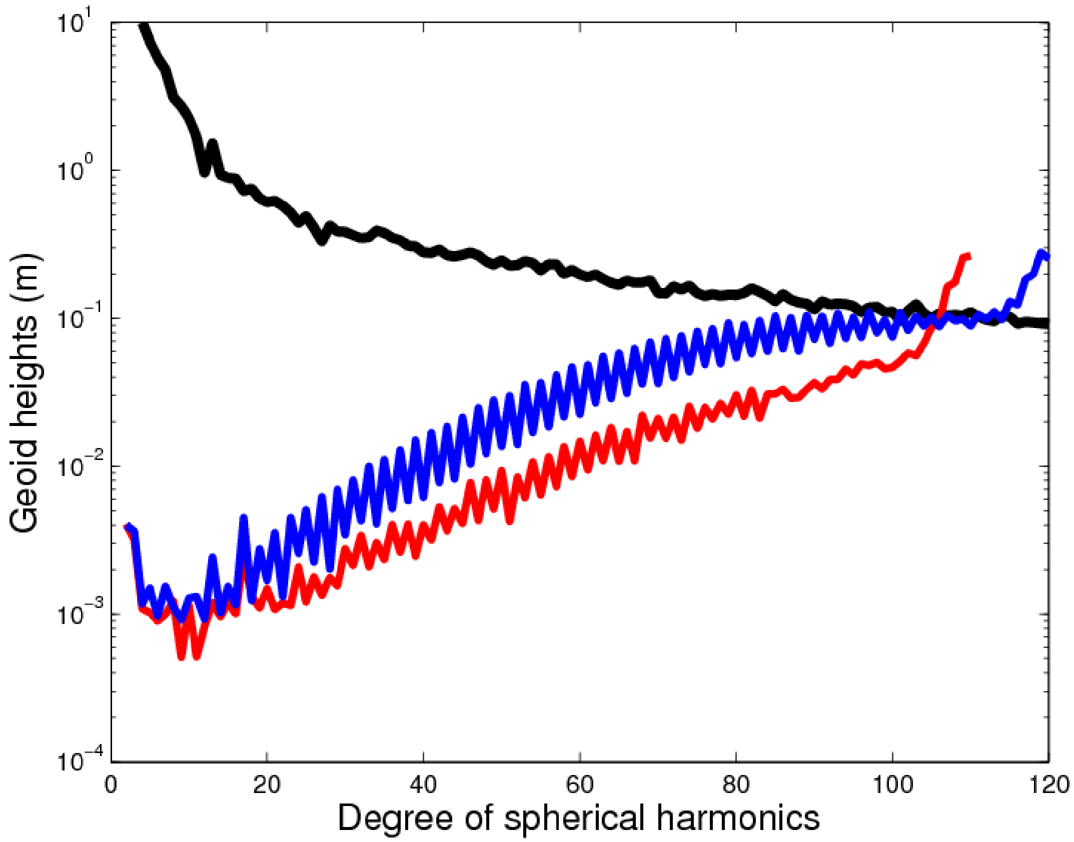

Reference field:

ITG-GRACE03S

Differences:

n_{max} = 110

n_{max} = 120

Differences seem to become significantly larger when increasing the parameter space …

Impact of the Polar Gap (2)

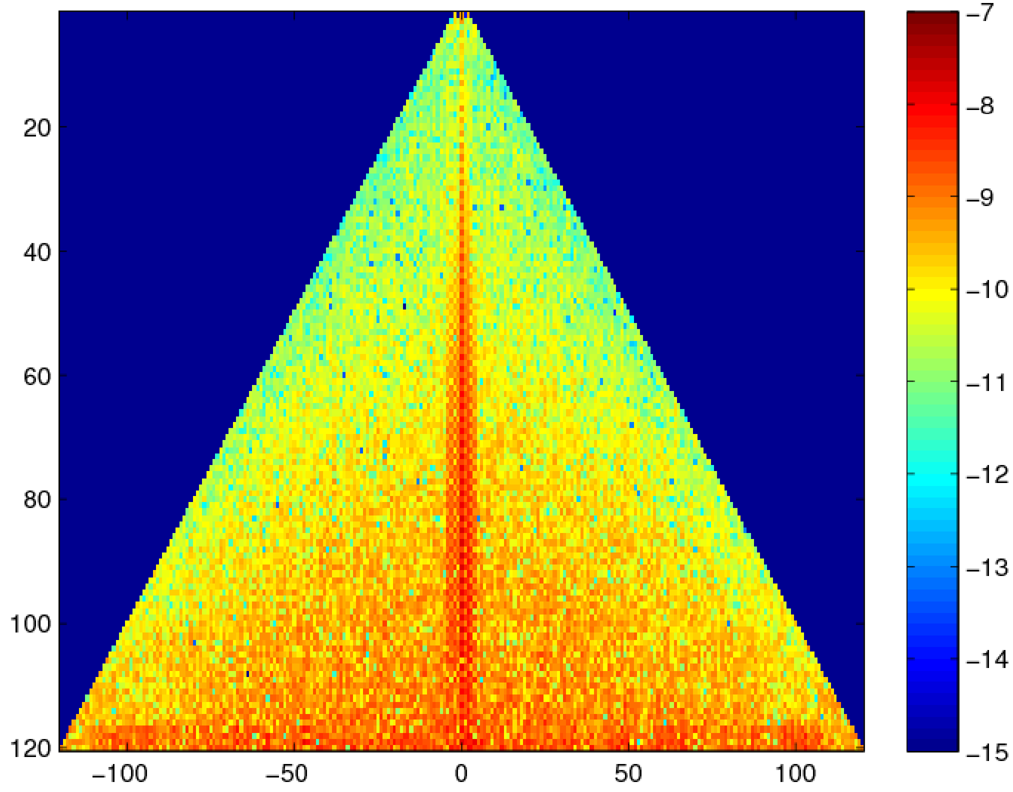

Max. Deg.:

n_{max} = 90

n_{max} = 110

n_{max} = 120

Zonal terms are weakly estimated (polar gap) and suffer when increasing the parameter space

Selection of the Maximum Degree

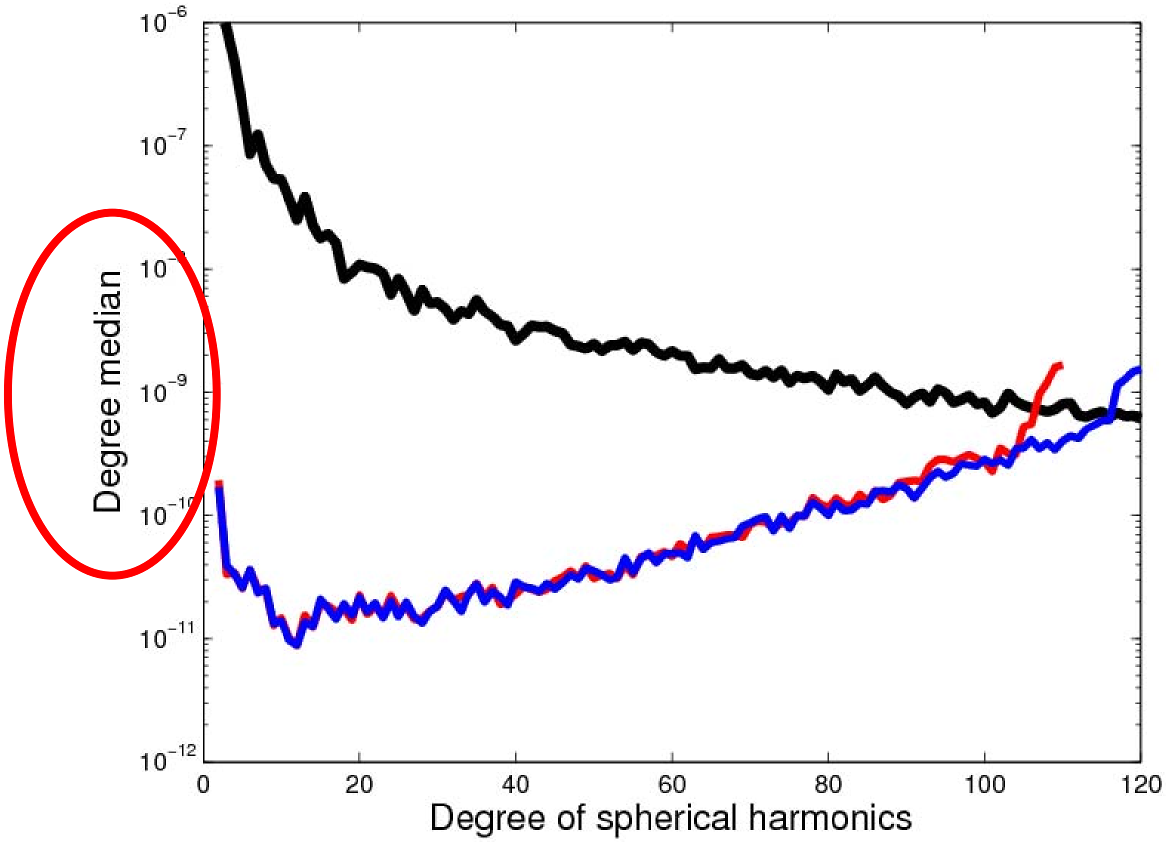

Reference field:

ITG-GRACE03S

Differences:

$n_{max} = 110$

$n_{max} = 120$

A maximum degree larger than 120 should be used when longer data spans will be processed

Impact of PCVs on gravity field recovery

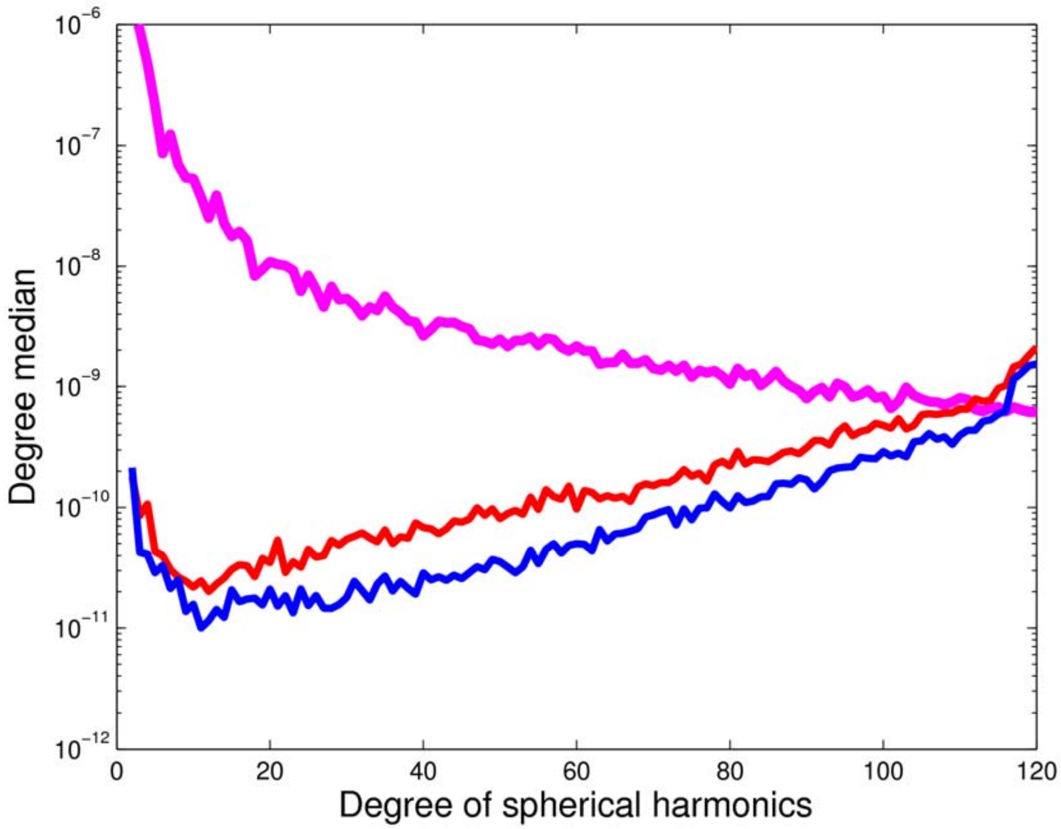

Reference field:

ITG-GRACE2010

Differences:

GOCE (w/o PCV)

GOCE (with PCV)

Unmodelled PCVs significantly contribute to the error-budget of GPS-only gravity field recovery

Contribution to Gradiometer Solutions

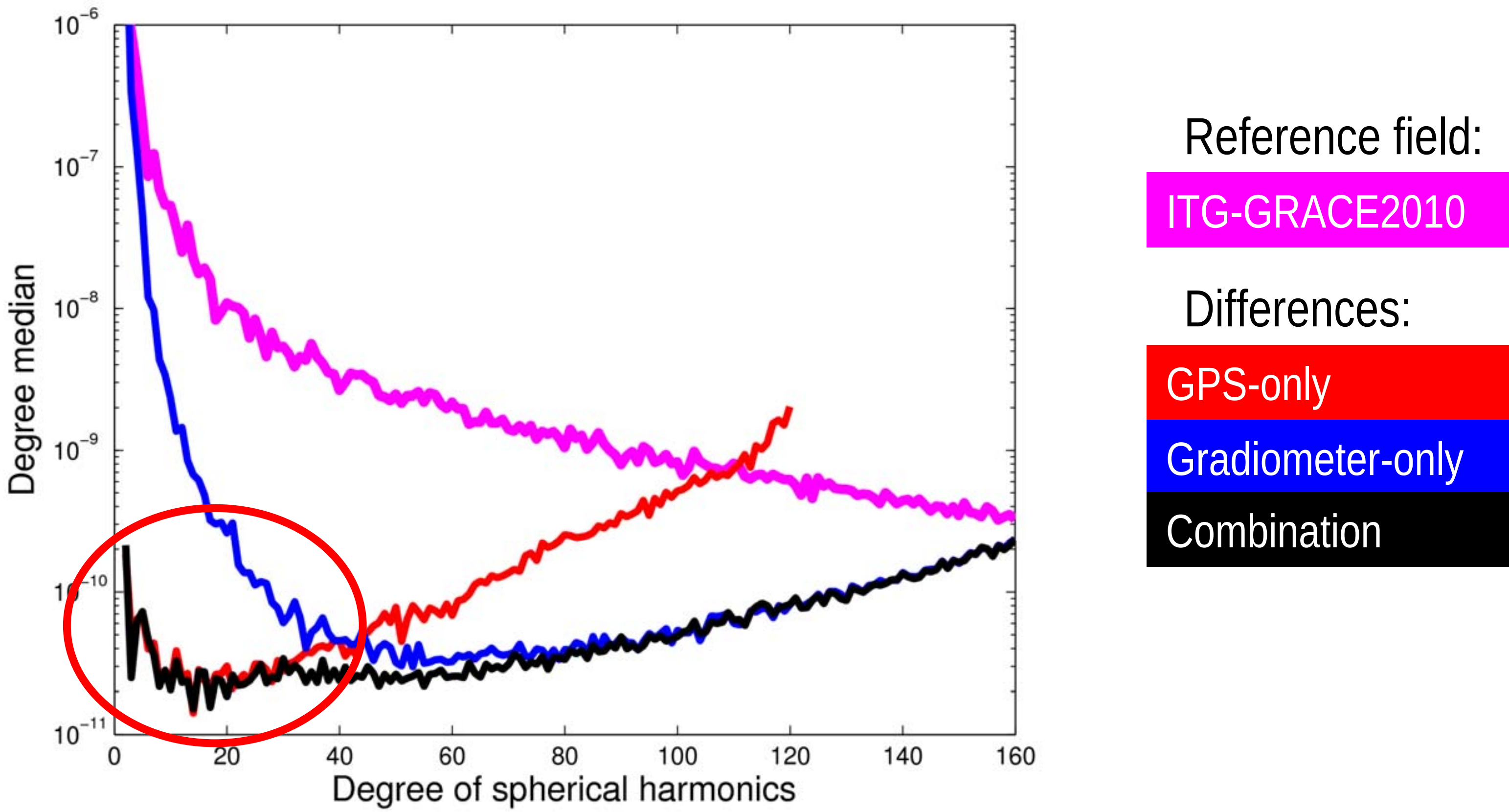

GPS contributes up to about degree 30 to combined GOCE-only gravity field solutions

Literature (1)

Blewitt, G. (1997): Basics of the GPS Technique: Observation Equations, in *Geodetic Applications of GPS*, Swedish Land Survey, pp. 10-54, available at http://www.sbg.ac.at/mat/staff/revers/lectures/2006_2007/GPS/GPSBasics.pdf

Bigazzi, A., B. Frommknecht (2010): Note on GOCE instruments positioning, XGCE-GSEG-EOPG-TN-09-0007, Issue 3.1, European Space Agency, available at http://earth.esa.int/download/goce/GOCE-LRR-GPS-positioning-Memo_3.1_[XGCE-GSEG-EOPG-TN-09-0007%20v3.1].pdf

Bock, H., A. Jäggi, D. Švehla, G. Beutler, U. Hugentobler, P. Visser (2007): Precise orbit determination fort he GOCE satellite using GPS. *Advances in Space Research*, 39(10), 1638-1647, doi: 10.1016/j.asr.2007.02.053

Bock, H., R. Dach, A. Jäggi, G. Beutler (2009): High-rate GPS clock corrections from CODE: Support of 1 Hz applications. *Journal of Geodesy*, 83(11), 1083-1094, doi: 10.1007/s00190-009-0326-1

Dach, R., E. Brockmann, S. Schaer, G. Beutler, M. Meindl, L. Prange, H. Bock, A. Jäggi, L. Ostini (2009): GNSS processing at CODE: status report, *Journal of Geodesy*, 83(3-4), 353-366, doi: 10.1007/s00190-008-0281-2

Literature (2)

GOCE Standards (2009): GO-TN-HPF-GS-0111, Issue 3.1. European GOCE Gravity Consortium, available at http://earth.esa.int/pub/ESA_DOC/GOCE/GOCE_Standards_3.1.pdf

GOCE Level 2 Product Data Handbook (2009): GO-MA-HPF-GS-0110, Issue 4.1. European GOCE Gravity Consortium, available at http://earth.esa.int/pub/ESA_DOC/GOCE/Product_DATA_Handbook_4.1.pdf

Jäggi, A., U. Hugentobler, G. Beutler (2006): Pseudo-stochastic orbit modeling techniques for low-Earth satellites. *Journal of Geodesy*, 80(1), 47-60, doi: 10.1007/s00190-006-0029-9

Jäggi, A. (2007): Pseudo-Stochastic Orbit Modeling of Low Earth Satellites Using the Global Positioning System. *Geodätisch-geophysikalische Arbeiten in der Schweiz*, 73, Schweizerische Geodätische Kommission, available at http://www.sgc.ethz.ch/sgc-volumes/sgk-73.pdf

Jäggi, A., H. Bock, R. Pail, H. Goiginger (2008): Highly Reduced-Dynamic Orbits and their Use for Global Gravity Field Recovery: A Simulation Study for GOCE, *Studia Geophysica et Geodaetica*, 52(3), 341-359, doi: 10.1007/s11200-008-0025-z

Literature (3)

Jäggi, A., G. Beutler, L. Prange, R. Dach, L. Mervart (2009a): Assessment of GPS-only observables for Gravity Field Recovery from GRACE, in *Observing our Changing Earth*, edited by M. Sideris, pp. 113-123, Springer, doi: 10.1007/978-3-540-85426-5_14

Jäggi, A., R. Dach, O. Montenbruck, U. Hugentobler, H. Bock, G. Beutler (2009b): Phase center modeling for LEO GPS receiver antennas and its impact on precise orbit determination. *Journal of Geodesy*, 83(12), 1145-1162, doi: 10.1007/s00190-009-0333-2

Svehla, D., M. Rothacher (2004): Kinematic Precise Orbit Determination for Gravity Field Determination, in *A Window on the Future of Geodesy*, edited by F. Sanso, pp. 181-188, Springer, doi: 10.1007/b139065

Visser, P., J. van den IJssel, T. van Helleputte, H. Bock, A. Jäggi, G. Beutler, D. Švehla, U. Hugentobler, M. Heinze (2009): Orbit determination for the GOCE satellite, *Advances in Space Research*, 43(5), 760-768, doi: 10.1016/j.asr.2008.09.016.